Contrails

INHIBITION OF FLOW SEPARATION AT HIGH SPEED

VOL. III. — EXPERIMENTAL RESULTS FOR LAMINAR BOUNDARY LAYERS

JACK N. NIELSEN
LARRY L. LYNES
FREDERICK K. GOODWIN

This document has been approved for public release and sale; its distribution is unlimited.

Approved for Public Release

Contrails

FOREWORD

This report,[1] "Inhibition of Flow Separation at High Speed, Vol. III - Experimental Results for Laminar Boundary Layers," represents the third in a series of technical reports concerned with inhibiting separation of laminar and turbulent boundary layers at supersonic speeds. The work was carried out by Nielsen Engineering & Research, Inc., 3967 East Bayshore, Palo Alto, California 94303, under Contract No. F33615-67-C-1096. The contract was initiated under Project 8219, Task 821902 of the Air Force Flight Dynamics Laboratory (AFFDL) and was funded in part by Laboratory Director Funds. The technical monitor of the contract was Mr. Eugene L. Fleeman (FDCC). The research started on October 14, 1966, and this phase of the work is effectively concluded with the date of submission of this report, August 16, 1968.

The authors wish to thank Mr. J. Don Gray of ARO, Inc., who acted as project engineer for the wind-tunnel testing at the von Karman Facility, Arnold Engineering Development Center (AEDC), Tullahoma, Tennessee.

The authors also wish to thank Mr. Eugene L. Fleeman who has helped overcome both technical and administrative problems during the course of the work.

This manuscript was released by the authors in August 1968 as an AFFDL technical report.

This technical report has been reviewed and is approved.

C. B. Westbrook, Chief
Control Criteria Branch
Flight Control Division

[1] This is Nielsen Engineering & Research, Inc., Report TR 9.

Approved for Public Release

Contrails

ABSTRACT

This report is the third in a series of reports on the subject of inhibition of separation at high speed. It describes the results of a wind-tunnel test program carried out at the von Karman Facility of the Arnold Engineering and Development Center at Tullahoma, Tennessee, on an ogive-cylinder-flare combination to determine the extent of laminar separation as a function of wall temperature for fixed free-stream Reynolds number per unit length at a free-stream Mach number of 8.0. The objective of the tests was to see if separation could be eliminated entirely by cooling the wall to a sufficiently low value.

Pressure and temperature distributions spanning the separation region were taken on a quick-insertion model, but the location of the separation point could not be obtained during the tests. Accordingly, a combined experimental-theoretical method was developed for determining the separation point location. Correlation of the separation length with model to free-stream temperature ratio indicated that the separation distance was small and was rapidly approaching zero at the lowest temperature ratio achieved experimentally. The apparent critical temperature ratio so indicated by the data was lower than the theoretical ratio. It was not possible to achieve sufficiently low temperatures to see if separation could be entirely eliminated. Possible reasons for the difference between experiment and theory are discussed.

Approved for Public Release

Contrails

Approved for Public Release

Contrails

TABLE OF CONTENTS

Approved for Public Release

Contrails

TABLES

ILLUSTRATIONS

Approved for Public Release

Contrails

ILLUSTRATIONS (Conc.)

Approved for Public Release

Contrails

LIST OF SYMBOLS

c_p	specific heat of air at constant pressure
D	diameter of cylindrical section of ogive-cylinder-flare combination
k	thermal conductivity of air
L	axial distance from nose of body to beginning of interaction (fig. 1)
L_c	axial distance from nose to cylinder-flare juncture
L'_E	distance from virtual origin of laminar boundary layer to beginning of interaction
M_o	edge Mach number at beginning of interaction
M_∞	free-stream Mach number
p	local static pressure at wall
p_i	static pressure at inflection point
p_o	static pressure at edge of boundary layer at beginning of interaction
p_s	static pressure at separation point
p_{t_∞}	wind-tunnel stagnation pressure
p_∞	wind-tunnel, free-stream, static pressure
$p_1, p_2, \cdots$	static pressure at orifice nos. 1,2,$\cdots$ (fig. 1)
Pr	Prandtl number, $\mu c_p/k$
Re_o	Reynolds number at beginning of interaction, $u_o \rho_o L'_E/\mu_o$
Re_∞/ft	free-stream Reynolds number per foot
r	radius of ogive nose
s	axial distance along surface of ogive-cylinder-flare combination taken positive behind cylinder-flare juncture
T_{cr}	critical wall temperature
T_r	recovery temperature
T_{t_∞}	free-stream total temperature
T_w	wall temperature
$\overline{T}_w$	average of T_1, T_2, and T_3

Approved for Public Release

Contrails

T_1, T_2, T_3	model local temperatures measured in tests
u_o	fluid velocity at edge of boundary layer at beginning of interaction
x	axial distance positive downstream from model nose
x'	axial distance positive downstream of virtual origin of laminar boundary layer
x_i	value of x at inflection point
x_o	value of x at beginning of interaction
x_s	value of x at separation
x'_s	value of x' at separation
μ	absolute viscosity of air
ρ	mass density of air

Subscripts

cr	critical
i	inflection point
o	beginning of interaction
s	separation
∞	free stream

Approved for Public Release

Contrails

Approved for Public Release

Contrails

INHIBITION OF FLOW SEPARATION AT HIGH SPEED

VOL. III - EXPERIMENTAL RESULTS FOR LAMINAR BOUNDARY LAYERS

1. INTRODUCTION

This report is the third in a series describing an investigation of the inhibition of boundary-layer separation at high speeds through the use of surface cooling. References 1 and 2 are the first and second parts of the series. Former theoretical works, references 3, 4, and 5, indicate the possibility of eliminating laminar separation controlled by free interaction by cooling the wall surface below its critical temperature. Specifically it was found that for Blasius-type initial conditions the amplification process represented by free interaction between the boundary layer and the outer flow, which usually results in separation, becomes a damping process below a certain critical temperature ratio dependent on Mach number and specific heat ratio. This result implies either that separation is eliminated, or if it occurs, it is not of the usual free-interaction type. It is important that the initial conditions at the beginning of interaction be of the Blasius type, and that the interaction between the inner and outer flows be of the free-interaction type with isentropic conditions at the edge of the boundary layer. As a result of the theoretical prediction, the Air Force Flight Dynamics Laboratory sponsored the present investigation to extend the theory and to perform experimental work. The specific purpose of this report is to present the experimental results.

There has been very little previous data suitable for establishing the existence or nonexistence of the critical temperature ratio because great care must be taken to maintain uniform but variable surface temperature. One set of data taken by Ryder (ref. 6) in a hypersonic shock tunnel for a cone-flare configuration has been analyzed by Fleeman (ref. 7) to determine the possible existence of a critical temperature ratio. The run time of a few milliseconds was not long enough to cause appreciable nonuniform surface temperature, and the skin-friction gauges yielded positive indications of separation. Fleeman found a critical temperature ratio in the data of Ryder, but its value was less than the predicted value. Another set of data taken by Lankford (refs. 8, 9, and 10) for an axisymmetric compression surface which is conical over most of its length shows that laminar separation was "almost eliminated by cooling the wall." The data were obtained both in a wind tunnel and a firing range.

Approved for Public Release

Contrails

In the present investigation an ogive-cylinder-flare combination was tested at hypersonic speed in Tunnel B of the von Karman Facility of the AEDC at Tullahoma, Tennessee, to determine the length of laminar separated flow as a function of model surface to free-stream temperature ratio. The model was cooled by spraying it with liquid nitrogen. Pressure orifices were closely spaced in the expected region of separation, and the pressures were recorded repeatedly during short runs with fast-response instrumentation. Model temperatures were similarly recorded. The presentation and analysis of the data constitute the principal purpose of this report.

2. DESCRIPTION OF THE EXPERIMENT

2.1 General Approach

In executing the present experiment, special problems were anticipated in determining the location of separation on highly-cooled wall surfaces and in maintaining the model at uniform but variable surface temperature. It was decided not to use an internally-cooled model in a continuous wind tunnel because of the conflicting requirements of using the internal volume for cooling channels, pressure lines, and other instrumentation. Rather it was decided to use an externally cooled quick-insertion model with fast-response pressure instrumentation which could yield pressure data before the model temperature could rise significantly. Within the short run times, of the order of a few seconds, simple means were not found to locate the separation point experimentally with the model surface near the temperature of liquid nitrogen. Heat-transfer gauges were installed in the model to determine whether or not the flow was fully laminar. An indication of boundary-layer transition should follow from any change in the slope of the plot of Stanton number versus Reynolds number on log-log paper. In order not to disturb the boundary layer at the nose-cylinder juncture, an ogive nose rather than a conical nose was utilized. A fairly long length of cylindrical section was included in the body to produce Blasius-type conditions at the beginning of interaction.

2.2 Model Description

A drawing of the model is shown in figure 1. It consists of an ogive nose 3 inches long, a cylindrical section 6.8 inches long, and a frustrum of a 10° cone with a slant height of 6 inches. The nose, Agard Model B, is an ogive of fineness ratio 3 with a shape given by

Approved for Public Release

Contrails

$$\left(\frac{r}{D}\right) = \frac{1}{3}\left(\frac{x}{D}\right) - \frac{1}{27}\left(\frac{x}{D}\right)^3 + \frac{1}{162}\left(\frac{x}{D}\right)^4 \qquad (1)$$

where

r = local radius of ogive

D = diameter at base of ogive = 1.0 inch

x = axial distance from ogive vertex

There are a total of 41 pressure taps placed in the model with a spacing of 0.1 inch in the region of the cylinder-flare juncture and a broader spacing at greater distances from the juncture. The surface positions of the orifices are given in Table I.

There are also three thermocouples which were originally mounted on the cover plate of the model. Preliminary testing showed that repeatable pressure and temperature data could not be obtained with the thermocouples on the cover plate. They were reinstalled in the main copper body just under the surface, and repeatable data as a function of model temperature were obtained.

Of the three heat-transfer gauges two were installed on the flare in positions such that at least one should generally be downstream of reattachment. During the tests the heat-transfer gauges were inoperative so that other means had to be used to determine whether the flow was fully laminar. Shadowgraphs of flow reattachment indicated fully laminar flow for the tests.

2.3 Measuring Instrumentation

The fast-response pressure system specifically developed to meet the requirements of tests such as the present one is described in references 11 and 12. The transducer package had controlled internal pressure and temperature, and the transducer package pressure acted as the reference pressure for the transducers, each of which was connected to an orifice. The pressure data were recorded on magnetic tape in digital form. Chromel-alumel thermocouples were used to measure the model temperature.

During the testing the zero of each transducer was recorded at the beginning and end of each run. When the zero shifts were small, the measurements were repeatable to ± 0.002 psi. Temperatures were repeatable to well within 1°, and the model temperatures were generally uniform within the test range as shown in Table II.

Approved for Public Release

Contrails

2.4 Testing Procedure

The model was cooled in position in the injection tank by spraying it from manifolds on both sides of the model. To avoid frosting for low model surface temperatures, the spraying was done with the tank pressure close to free-stream static pressure. Also an air jet was used to control frosting. When the thermocouples indicated uniform model temperature at the desired level, the model was injected into the wind tunnel through doors. Pressure and temperature levels were recorded continuously.

Time histories of the pressure readings for several orifices at two pressure levels are shown in figure 2. Figure 2(a) shows typical data for the lowest tunnel stagnation pressure of the tests, a nominal value of 150 psia, and figure 2(b) corresponds to the highest stagnation pressure, a nominal value of 600 psia. The forward pressure, p_1, the pressure near the cylinder-flare juncture, p_{15}, and the pressure on the flare, p_{30}, all show fairly constant values near the end of the run for the low pressure case, figure 2(a). The last pressure printout is the one presented as data herein except for a few isolated points where the last point was clearly inaccurate. At the higher total pressure, figure 2(b) shows essentially constant pressure except on the flare where the random pressure variations are greater than for the other points. The latter variations are, nonetheless, within acceptable limits.

Time histories of the three model temperatures are shown in figure 3(a) for a tunnel stagnation pressure of 150 psia and in figure 3(b) for a stagnation pressure of 600 psia. The forward model temperature T_1 does not rise as rapidly as the rear temperature T_3. The intermediate temperature in the separation zone shows some irregularity in its rate of temperature rise. However, the model temperatures were generally within a $\pm 5^{\circ}$ F spread by the time the final data are recorded. The low rate of model temperature rise and the uniformity of model temperature were considered adequate for the purposes of the investigation.

3. PRESENTATION OF DATA

A large number of runs were made at a nominal Mach number of 8.0, and a few runs were made at a nominal Mach number of 6.0. Only the Mach number 8.0 data are presented here because the data for the lower Mach number are all above the theoretical critical temperature ratio. While approximately 183 runs were made at $M = 8$, only about 50 are presented here as prime data.

Approved for Public Release

Contrails

Prime data have been selected on the basis that the model temperature differences and the zero shift of the pressure transducers are within certain limits. How the model is cooled with liquid nitrogen and how long it has "soaked" to attain thermal equilibrium before injection will determine its uniformity of temperature. A nominal spread of $\pm 5^{\circ}$ F from the mean of the three model temperatures was taken as the allowable model temperature difference for prime data. This spread means a variation in T_w/T_{t_∞} of about ± 0.004 for a stagnation temperature of 1250° R. If the zero shifts for the pressure transducers were less than 10^{-3} psi for all but a few of the transducers, the data for the run were accepted as prime data. A zero shift of 10^{-3} psi corresponds to a 6 percent error for a pressure equal in magnitude to the free-stream static pressure for a tunnel stagnation pressure of 150 psi, whereas it means an error of only about 1.5 percent at 600 psi.

In addition to the criteria for prime data, criteria were also specified for marginal data. The marginal data consist of any data not prime data for which the zero pressure shifts for a given run were all less than 0.005 psi, and the model temperature differences were $\pm 5^{\circ}$ or less.

Based on the foregoing criteria, about 50 runs were selected as prime data and about 70 runs were selected as marginal data out of a total number of 183 runs. The prime data are presented in Table II. The data are arranged primarily in ascending order of tunnel stagnation pressure and secondarily in ascending order of temperature ratio. Four nominal tunnel stagnation pressures of 150, 300, 450, and 600 psia were used in the tests. Model temperatures varied from that of liquid nitrogen to ambient temperatures. First the tunnel total pressure, total temperature, and Mach number are presented, then the free-stream Reynolds number per foot is presented together with the three model temperatures. The pressure data are presented in the form p/p_∞ for 39 of the 41 pressure orifices. The orifices at values of s equal to 1.7 inches and 2.3 inches were inoperative during the tests.

For comparison with theory the pressure distributions are usually required in the form p/p_o, where p_o is the uniform pressure preceding the beginning of interaction. The value of p_o/p_∞ for the present tests varies with Reynolds number and temperature ratio, probably as a result of boundary-layer displacement effects. The value of p_o/p_∞ was determined from the tabulated data, and the conversion from p/p_∞ to p/p_o was made for purpose of comparison between experiment and theory.

Approved for Public Release

Contrails

4. RESULTS AND DISCUSSION

4.1 Determination of Separation Point Location

Some significant aspects of the separated flow and its associated pressure distribution are shown in figure 4. The significant points are the beginning of interaction designated by O; the inflection point in the pressure distribution designated by i, and the separation point designated by S. The boundary layer at O corresponds to a Reynolds number Re_o based on edge conditions at O and a boundary layer run L'_E from a virtual origin O'. Up to the beginning of the flare-cylinder juncture, the behavior of the boundary layer on the cylinder is two dimensional.

Since it was not possible to determine the separation point location experimentally during the present tests, other means of determining the location have been devised. In reference 13, Kuehn gives as the criterion for the existence of separation the appearance of three points of inflection in the pressure distribution. It is known that the separation point occurs near the first inflection point. Since an inflection point in the pressure distribution is a geometrically distinguishable point, it can be used as a first approximation to the separation point location. To this experimentally determined inflection point position a small adjustment can be added to account for the difference between inflection point and separation point locations. The adjustment is a theoretical one obtained from a theoretical solution which is specially fitted to the experimental pressure distribution as described in the Appendix. At a tunnel stagnation pressure of 150 psi, it is difficult to determine the inflection point, so that no correlation of separation point location will be made for the lowest tunnel stagnation pressure.

In fitting the theory of reference 2 to the experimental pressure distribution, the values of M_o and T_w/T_{t_∞} are known from the data. A value of initial Reynolds number is chosen such that the slope of the pressure distribution at the inflection point is matched. The first step in the matching process is to establish a theoretical curve of the parameter $L'_E(d/dx)(p/p_o)_i$, the nondimensional pressure gradient at the inflection point, versus Re_o for fixed M_o and T_w/T_{t_∞} using the computer program of reference 2. With this curve and the experimental value of $(d/dx)(p/p_o)_i$, it is possible to determine the value of L'_E which will put the theoretical and experimental slopes into agreement. The displacement between the inflection point and the separation point can then be determined from the computer

Approved for Public Release

Contrails

program since the nondimensional distance $(x_s - x_i)/L'_E$ is a function only of Re_o, M_o, and T_w/T_{t_∞}.

In order to make sure the theoretical fitting technique yielded good results, a series of 14 data runs were selected for a range of tunnel stagnation pressures and wall temperature ratios for comparison with the theoretical predictions. The basic parameters of the runs are shown in Table III. It is noted that the conditions at the beginning of interaction cover the range of tunnel stagnation pressure used in the tests. The initial Mach number, M_o, was calculated in the following manner. From the experimental values of the free-stream Mach number and stagnation pressure, the static pressure and stagnation pressure just behind the bow shock were obtained from cone tables. The semiapex angle of the tip of the ogive nose is 18.417^o. The static pressure at the edge of the boundary layer was then assumed to drop isentropically to the uniform value measured on the cylindrical section of the model in the neighborhood of the beginning of interaction. In this fashion the edge Mach number M_o is determined accounting for the boundary-layer displacement effects which are neglected in inviscid theory. In fact, the variation of M_o with tunnel stagnation pressure in Table III is believed due to such displacement effects.

From the values of edge Mach number and stagnation pressure at the beginning of interaction, the edge Reynolds number per unit length can be calculated. The value of Re_o, the Reynolds number at the beginning of interaction, is not known because the location of the virtual origin of the boundary layer is unknown. However, by varying Re_o in the computer program of reference 2 until the theoretical and experimental pressure distribution slopes match at the inflection point, the approximate value of Re_o can be obtained. From Re_o and the Reynolds number per unit length the distance between the virtual origin and the beginning of interaction, L'_E, is determined.

So far the position of the beginning of interaction has not been tied down. This can be done by making the theoretical and experimental inflection points coincide. The theoretical pressure distribution is thereby tied into the body coordinate system, and the theoretical positions of the beginning of interaction, separation point, and reattachment point in body coordinates can be located. In this fashion the distance L from the body nose to the beginning of interaction is determined.

In the actual fitting of the theory to the experimental pressure distributions, L'_E and L were independently varied by trial and error to

Approved for Public Release

Contrails

obtain the best possible fit. The final values of L_E' and L are those listed in Table III. A comparison between the theoretical and experimental pressure distributions is shown in figures 5(a) to 5(n). The closeness of the fit is sufficiently good for the purposes of establishing the theoretical values of $x_s - x_i$. The pressure distributions are shown only for the separation regions since the fits in these regions are the matters of interest here. Included in the figures are the theoretical positions of the beginning of interaction, the separation point, and the reattachment point. The theoretical positions include any inaccuracies in fitting the experimental data as well as any inaccuracies in the theory itself.

In Table III the experimental values of x_i have been listed for all 14 cases as well as the values of $x_s - x_i$ taken from the theoretical pressure distributions. The "experimental" values of x_s are obtained by adding the theoretical values of $x_s - x_i$ to the experimental values of x_i. It is noted that the values of $x_s - x_i$ represent only a small correction to the position of separation. The experimental values of x_s are close to the theoretical values but do not coincide with them because of the inaccuracies mentioned above.

4.2 Correlation of Inflection Point and Separation Point Locations

It has been possible to correlate the experimental data to obtain plots of separation distance as a function of temperature ratio for fixed Reynolds number. It is first to be noted in figure 5 that the separation and reattachment points are approximately the same distance upstream and downstream of the corner, especially for short overall separation distances. Thus, separation disappears when the separation point is exactly at the cylinder-flare juncture. A convenient nondimensional measure of the length of separated flow in front of the corner is $(L_c - x_s)/L_c$. In presenting the correlation, we will first show $(L_c - x_i)/L_c$, a purely experimental quality, and then $(L_c - x_s)/L_c$ determined as described previously.

The values of $(L_c - x_i)/L_c$ are plotted in figure 6 versus wall temperature ratio for the three highest tunnel total pressures using only the prime data. The comparison for $p_{t_\infty} = 150$ psia is missing because inflection points were hard to locate in the data. Data at finer intervals or more precise data may have shown well-defined inflection points. Despite the lack of such inflection points in the data for $p_{t_\infty} = 150$ psia (figs. 5(a), 5(b), and 5(c)) it is believed separation occurred because the theoretical curves which fit the data well and have inflection points indicate

Approved for Public Release

Contrails

separation. There is a clear trend of decreased nondimensional distance with decreased wall temperature ratio. The prime data at p_{t_∞} = 300 psia and 450 psia are rather sparse, but the data for p_{t_∞} = 600 psia show that the distance from the inflection point to the corner decreases more rapidly with cooling as the wall temperature is lowered. The data suggest a critical temperature ratio at some value of $\overline{T}_w/T_{t_\infty}$ less than 0.103, the lowest measured.

In order to see how the marginal data might affect the conclusion of the preceding paragraph, correlation plots similar to those in figure 6 were made using both prime data and marginal data. These new plots are presented in figure 7. The conclusions reached on the basis of figure 6 are unchanged although the somewhat greater scatter due to the marginal data is evident.

A correlation is presented in figure 8 of the nondimensional distance from the separation point to the corner. The prime data and marginal data are both included in the correlation for tunnel stagnation pressures of 300, 450, and 600 psia. The data at 600 psia again show a tendency toward zero separation distance from the corner as $\overline{T}_w/T_{t_\infty}$ decreases towards its lower experimental limit of 0.103. It cannot be said whether separation would be eliminated if $\overline{T}_w/T_{t_\infty}$ had decreased slightly more, and in this sense the results are inconclusive. It has been determined that the apparent critical temperature ratio in this case is less than 0.103 which is well below the value of 0.162 predicted for M_o = 6.8 by the theory of reference 2. It is more nearly in agreement with a value of 0.13 found by Fleeman in reference 7.

4.3 Reasons for Deviation Between Theory and Experiment

In comparing the quantitative results for the critical temperature ratio, several points should be kept in mind. For M_o of 6.8 the predicted ratio of T_{cr}/T_{t_∞} = 0.162 is based on a Prandtl number of unity, whereas for air the Prandtl number is less than unity. The effect on the critical temperature ratio of a Prandtl number different from unity might be estimated by assuming that the ratio T_{cr}/T_r is the proper experimental parameter to compare with the theoretical value of T_{cr}/T_{t_∞}. On this basis an experimental value of T_{cr}/T_{t_∞} of 0.103 would correspond to a value of T_{cr}/T_r of 0.134. This latter value of 0.134 is then comparable with the theoretical value of T_{cr}/T_{t_∞} = 0.162 for a Prandtl number of unity.

Another point of possible inaccuracy in the theoretical value of T_{cr}/T_{t_∞} might be due to an insufficient number of parameters in the velocity-profile representation used in the theory of reference 2. While convergence was apparently demonstrated in that reference with regard to

Approved for Public Release

Contrails

the number of arbitrary constants in the temperature profile, the addition of another parameter in the velocity profile to demonstrate convergence on that score was not carried out. It is possible to take account in the theory of Prandtl numbers different from unity and of additional parameters in the velocity-profile representation.

5. CONCLUDING REMARKS

A wind-tunnel test program has been carried out on an ogive-cylinder-flare configuration to determine the extent of laminar boundary-layer separation as a function of wall temperature for fixed tunnel Reynolds number per unit length and fixed tunnel Mach number. The objective of the tests was to see if separation could be eliminated by cooling the wall temperature to a sufficiently low value.

The pressure and temperature measurements were made on a quick-insertion model, however, the separation point location could not be determined experimentally. Consequently, a combined experimental-theoretical method of determining the separation point location was developed. Correlation of the separation distance with model temperature ratio indicates that the separation distance was small and rapidly approached zero at the lowest wall temperature ratio achieved experimentally. It was not possible to achieve the temperature ratio, T_w/T_{t_∞}, less than 0.103 needed to see if separation could be totally eliminated.

The theoretical critical value of T_w/T_{t_∞} was 0.162 for the Mach number at the beginning of interaction of 6.8 and a Prandtl number of unity. The apparent experimental value of the critical temperature ratio was 0.103 or less. Part of the difference can be ascribed to the fact that the test Prandtl number was different from unity. Also, convergence of the theory with regard to the number of parameters (four) used in the velocity-profile representation has not been demonstrated. Both factors can be accounted for in the theory.

Some question exists as to whether the separation in a sharp interior corner can ever be completely eliminated because of the discontinuity in the streamline slope just at the corner. Tests with a slightly rounded corner could answer this question.

Approved for Public Release

Contrails

6. RECOMMENDATIONS FOR FUTURE WORK

The present experimental program has demonstrated that good separation data can be obtained near the critical temperature ratio with a quick-insertion copper model and fast-response pressure and temperature recording instrumentation. It has also demonstrated the apparent existence of a critical-temperature ratio. However, it would be desirable to repeat the tests to lower wall temperature ratios to see if laminar separation can be completely eliminated by wall cooling. It would be better to obtain lower temperature ratios by increasing tunnel stagnation temperature above that of the present tests because it is difficult to cool the model to temperatures below those of liquid nitrogen.

In further tests, it is probable a rounded juncture between the cylinder and flare should be used to eliminate possible questions of local separation in a sharp corner because of the discontinuity in shape of the wall streamline. Also, flare angles other than the present 10° flare should be tested. Generally speaking, very little systematic experimental information is available on laminar separation phenomena near the critical temperature ratio. Such information is needed to answer certain basic questions. Will separation be eliminated by cooling beneath the critical temperature ratio since free interaction with isentropic edge conditions will not cause pressure amplification? Will separation of another type (strong interaction) nevertheless occur? Is the subcritical-supercritical jump a limitation of theory or does it occur experimentally?

In addition to further experimental work, further analytical work is desirable. In particular, the critical temperature ratio results should be refined to account for Prandtl number other than unity. Also, higher approximations should be carried out in the theory for the velocity-profile representation to demonstrate convergence of the theory with regard to the number of parameters in the representation.

Approved for Public Release

Contrails

TABLE I

SURFACE POSITIONS OF PRESSURE ORIFICES AND THERMOCOUPLES

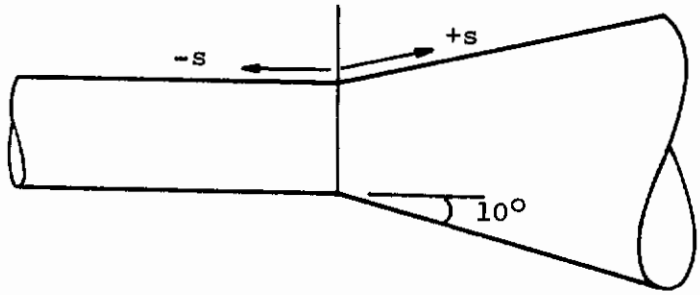

Thermocouple	s, in.
T_1	- 3.25
T_2	0.20
T_3	3.00

Orifice No.	s, in.	Orifice No.	s, in.	Orifice No.	s, in.
1	-3.5	15	-0.4	29	1.3
2	-3.0	16	- .3	30	1.5
3	-2.5	17	- .2	31	1.7
4	-2.3	18	- .1	32	1.9
5	-2.1	19	0.0	33	2.1
6	-1.9	20	.1	34	2.3
7	-1.7	21	.2	35	2.5
8	-1.5	22	.3	36	3.0
9	-1.3	23	.4	37	3.5
10	-1.1	24	.5	38	4.0
11	- .9	25	.6	39	4.5
12	- .7	26	.7	40	5.0
13	- .6	27	.9	41	5.5
14	- .5	28	1.1		

Approved for Public Release

Contrails

TABLE II

PRESSURE AND TEMPERATURE DATA FOR
OGIVE-CYLINDER-FLARE COMBINATION

	s, ins.	Run No. 1	2	3	4	5	6
Pt_∞, psia		155.3	152.8	153.6	148.8	151.9	151.1
M_∞		7.96	7.96	7.96	7.96	7.96	7.96
T_{t_∞}, °R		1184	1189	1191	1200	1190	1190
Re_∞/ft$\times 10^{-5}$		8.288	8.097	8.125	7.781	8.043	8.002
T_1, °R		261.2	347.7	347.5	533.7	530.1	534.8
T_2, °R		261.9	348.8	349.9	533.2	533.1	537.0
T_3, °R		262.5	349.1	350.8	533.0	534.8	537.1
p/p_∞	-3.5	1.050	1.094	1.096	1.089	1.085	1.076
	-3.0	1.049	1.059	1.076	1.032	1.069	1.075
	-2.5	1.073	1.091	1.101	1.075	1.067	1.097
	-2.3	1.052	1.098	1.093	1.020	1.051	1.041
	-2.1	1.105	1.133	1.108	1.063	1.074	1.100
	-1.9	1.032	1.073	1.043	1.021	--	--
	-1.7	1.060	1.085	1.061	1.033	1.068	1.074
	-1.5	1.088	1.115	1.091	1.055	1.074	1.089
	-1.3	1.058	1.076	1.063	1.063	1.068	1.046
	-1.1	1.057	1.107	1.069	1.059	1.091	1.070
	- .9	--	1.038	1.083	1.113	1.042	1.100
	- .7	--	1.092	1.099	1.092	1.115	1.134
	- .6	--	1.106	1.101	1.195	1.187	1.194
	- .5	1.103	1.161	1.169	1.246	1.270	1.270
	- .4	1.140	1.222	1.286	1.290	1.357	1.327
	- .3	1.254	1.349	1.361	1.410	1.408	1.415
	- .2	1.383	1.482	1.465	1.484	1.483	1.500
	- .1	1.505	1.560	1.589	1.509	1.581	1.560
	0.0	1.598	1.606	1.651	1.586	1.625	1.616
	.1	1.697	1.715	1.696	1.661	1.697	1.697
	.2	1.849	1.819	1.840	1.747	1.823	1.808
	.3	1.905	1.991	1.947	1.820	1.922	1.904
	.4	2.095	2.040	2.086	1.852	2.002	1.970
	.5	2.213	2.201	2.195	1.988	2.123	2.101
	.6	2.399	2.310	2.313	2.111	2.134	2.177
	.7	2.567	2.457	2.471	2.186	2.278	2.336
	.9	2.839	2.724	2.710	2.447	2.539	2.524
	1.1	3.181	2.917	3.072	2.656	2.486	2.604
	1.3	3.501	3.244	3.345	2.908	2.846	2.897
	1.5	3.583	3.488	3.435	3.036	3.209	3.190
	1.9	3.871	3.742	3.699	3.446	3.518	3.521
	2.1	3.969	3.832	3.776	3.538	3.607	3.607
	2.5	4.147	4.079	3.928	3.866	3.899	3.899
	3.0	4.211	4.098	4.049	4.000	4.099	4.093
	3.5	4.246	4.262	4.177	4.126	--	--
	4.0	4.292	4.307	4.277	4.283	--	--
	4.5	4.300	4.378	4.258	4.266	--	--
	5.0	4.406	4.397	4.323	4.366	--	--
	5.5	4.342	4.343	4.289	4.416	4.435	4.435

Approved for Public Release

Contrails

TABLE II

CONTINUED

	s, ins.	Run No. 7	8	9	10	11	12
p_{t_∞}, psia		151.8	157.0	297.7	299.2	299.1	301.9
M_∞		7.96	7.96	7.98	7.98	7.98	7.98
T_{t_∞}, ^oR		1180	1185	1255	1252	1250	1245
Re_∞/ft$\times 10^{-5}$		8.138	8.368	14.46	14.59	14.62	14.83
T_1, ^oR		562.9	568.2	147.9	167.3	177.2	265.6
T_2, ^oR		563.5	566.8	141.3	165.3	168.1	261.4
T_3, ^oR		562.6	565.6	144.5	163.9	169.8	263.7
p/p_∞	-3.5	1.037	1.058	1.023	1.010	.9958	1.010
	-3.0	1.043	1.057	1.024	1.018	1.002	1.026
	-2.5	1.039	1.038	1.026	1.029	.9995	1.008
	-2.3	1.041	1.020	.9945	1.027	1.023	.9970
	-2.1	--	1.092	1.015	1.024	1.019	1.014
	-1.9	1.011	--	1.033	1.042	1.053	1.036
	-1.7	1.018	1.026	1.029	1.018	1.015	.9986
	-1.5	1.005	1.040	1.030	1.042	1.009	.9896
	-1.3	1.063	1.056	1.021	1.044	1.019	1.048
	-1.1	1.033	1.040	1.029	1.044	1.021	1.027
	- .9	1.087	1.133	1.035	1.041	1.026	1.041
	- .7	1.119	1.197	1.048	1.039	1.019	1.072
	- .6	1.195	1.248	1.060	1.054	1.043	1.138
	- .5	1.267	1.333	1.105	1.127	1.120	1.263
	- .4	1.370	1.366	1.253	1.283	1.291	1.411
	- .3	1.416	1.453	1.404	1.419	1.413	1.482
	- .2	1.441	1.544	1.502	1.507	1.522	1.536
	- .1	1.583	1.550	1.598	1.604	1.586	1.622
	0.0	1.605	1.594	1.625	1.624	1.625	1.650
	.1	1.695	1.626	1.742	1.737	1.728	1.731
	.2	1.748	1.708	1.933	1.910	1.907	1.854
	.3	1.777	1.827	2.109	2.048	2.063	1.982
	.4	1.894	1.840	2.311	2.260	2.256	2.180
	.5	2.019	1.962	2.541	2.502	2.502	2.363
	.6	2.074	2.047	2.761	2.673	2.650	2.519
	.7	2.174	2.135	2.927	2.873	2.823	2.664
	.9	2.391	2.285	3.278	3.220	3.177	3.010
	1.1	2.525	2.383	--	3.379	3.143	3.113
	1.3	2.771	2.632	3.611	3.659	3.453	3.428
	1.5	2.985	2.874	3.841	3.836	3.819	3.728
	1.9	3.243	3.126	3.978	3.981	3.970	3.923
	2.1	3.369	3.245	3.993	3.990	4.020	3.983
	2.5	3.586	3.502	4.009	4.019	4.061	4.070
	3.0	3.891	3.764	4.101	4.072	4.123	4.141
	3.5	--	3.911	4.128	4.088	4.172	4.180
	4.0	4.211	4.082	4.142	4.165	4.186	4.197
	4.5	4.168	4.058	4.104	4.120	4.132	4.122
	5.0	4.252	4.160	4.154	4.197	4.190	4.198
	5.5	4.302	4.234	4.174	4.192	4.223	4.229

Approved for Public Release

Contrails

TABLE II

CONTINUED

	s, ins.	Run No. 13	14	15	16	17	18
p_{t_∞}, psia		301.9	303.8	303.0	303.0	301.6	302.2
M_∞		7.98	7.98	7.98	7.98	7.98	7.98
T_{t_∞}, ^oR		1251	1273	1250	1249	1246	1258
Re_∞/ft$\times 10^{-5}$		14.73	14.45	14.81	14.82	14.81	14.64
T_1, ^oR		269.8	337.6	359.6	369.0	535.5	539.2
T_2, ^oR		264.6	336.5	362.8	370.3	532.2	538.5
T_3, ^oR		267.7	336.5	364.2	370.1	532.0	538.0
p/p_∞	-3.5	1.014	1.049	1.013	1.026	1.011	1.033
	-3.0	.9946	1.041	1.005	1.007	1.023	1.022
	-2.5	.9965	1.051	1.003	1.021	1.017	1.035
	-2.3	.9975	1.044	1.019	1.002	1.032	1.030
	-2.1	1.016	1.036	1.023	1.022	1.035	1.020
	-1.9	1.086	1.045	1.046	1.066	1.075	1.066
	-1.7	1.012	1.055	1.002	1.016	1.012	1.031
	-1.5	1.025	1.058	.9988	1.017	1.029	1.038
	-1.3	1.016	1.048	1.008	1.024	1.045	1.028
	-1.1	1.028	1.051	1.027	1.026	1.069	1.058
	- .9	1.008	1.084	1.059	1.087	1.162	1.127
	- .7	1.066	1.158	1.150	1.170	1.278	1.257
	- .6	1.135	1.265	1.244	1.268	1.353	1.342
	- .5	1.274	1.378	1.370	1.362	1.422	1.426
	- .4	1.382	1.510	1.413	1.437	1.472	1.476
	- .3	1.476	1.546	1.505	1.512	1.535	1.525
	- .2	1.547	1.585	1.562	1.566	1.571	1.590
	- .1	1.600	1.660	1.586	1.617	1.612	1.626
	0.0	1.643	1.694	1.643	1.634	1.643	1.661
	.1	1.742	1.785	1.699	1.704	1.690	1.725
	.2	1.871	1.898	1.807	1.820	1.776	1.804
	.3	1.986	--	1.918	1.906	1.841	1.886
	.4	2.156	2.136	2.031	2.023	1.934	1.961
	.5	2.343	2.309	2.203	2.203	2.045	2.106
	.6	2.480	2.451	2.342	2.343	2.146	2.204
	.7	2.652	2.573	2.516	2.493	2.267	2.321
	.9	2.992	2.932	2.808	2.796	2.528	2.573
	1.1	3.038	3.104	2.930	2.874	2.602	2.735
	1.3	3.395	3.492	3.262	3.229	2.932	3.109
	1.5	3.696	3.706	3.566	3.561	3.244	3.326
	1.9	3.915	3.996	3.824	3.813	3.593	3.666
	2.1	3.970	4.038	3.863	3.891	3.683	3.751
	2.5	4.057	4.180	4.021	4.024	3.898	3.977
	3.0	4.145	4.289	4.172	4.181	4.092	4.177
	3.5	4.167	4.340	4.186	4.181	4.184	4.188
	4.0	4.213	4.389	4.232	4.242	4.245	4.300
	4.5	4.159	4.349	4.176	4.189	4.199	4.216
	5.0	4.214	4.389	4.249	4.255	4.277	4.273
	5.5	4.238	4.449	4.234	4.255	4.275	4.279

Approved for Public Release

Contrails

TABLE II

CONTINUED

	s, ins.	Run No. 19	20	21	22	23	24
p_{t_∞}, psia		302.6	299.7	300.3	449.1	449.8	449.6
M_∞		7.98	7.98	7.98	8.00	8.00	8.00
T_{t_∞}, ^oR		1254	1257	1255	1283	1279	1278
Re_∞/ft$\times 10^{-5}$		14.71	14.53	14.58	20.97	21.09	21.10
T_1, ^oR		542.5	562.1	564.7	153.3	178.4	263.5
T_2, ^oR		540.5	561.6	563.2	147.9	175.8	261.2
T_3, ^oR		540.1	561.4	562.3	151.1	178.2	266.6
p/p_∞	-3.5	1.019	1.045	1.041	.9526	.9719	.9656
	-3.0	1.049	1.041	1.024	.9571	.9670	.9905
	-2.5	1.034	1.031	1.047	.9709	.9809	.9770
	-2.3	1.030	1.044	1.051	.9752	.9848	.9911
	-2.1	1.036	--	--	.9818	.9924	.9850
	-1.9	1.072	1.101	1.067	1.049	.9907	--
	-1.7	1.046	1.033	1.052	.9963	.9978	.9940
	-1.5	1.054	1.026	1.043	.9911	.9982	.9846
	-1.3	1.050	1.054	1.065	1.011	1.008	1.014
	-1.1	1.083	1.086	1.146	1.002	1.014	1.015
	- .9	1.164	1.201	1.259	1.034	1.056	1.065
	- .7	1.288	1.314	1.385	1.244	1.243	1.253
	- .6	1.360	1.380	1.448	1.350	1.359	1.352
	- .5	1.434	1.456	1.483	1.433	1.437	1.434
	- .4	1.486	1.513	1.505	1.449	1.491	1.479
	- .3	1.539	1.535	1.554	1.501	1.520	1.532
	- .2	1.577	1.598	1.594	1.512	1.521	1.573
	- .1	1.632	1.605	1.615	1.513	1.553	1.597
	0.0	1.654	1.676	1.664	1.566	1.585	1.621
	.1	1.711	1.692	1.683	1.641	1.660	1.679
	.2	1.823	1.785	1.746	1.827	1.827	1.821
	.3	1.914	1.851	1.821	2.014	2.009	1.971
	.4	1.958	1.928	1.878	2.104	2.115	2.056
	.5	2.097	2.038	1.975	2.403	2.388	2.297
	.6	2.210	2.127	2.080	2.641	2.618	2.469
	.7	2.326	2.226	2.166	2.864	2.818	2.655
	.9	2.590	2.446	2.363	3.297	3.231	3.046
	1.1	2.826	2.613	2.648	3.496	3.474	3.278
	1.3	3.166	2.934	2.916	3.792	3.784	3.611
	1.5	3.345	3.139	2.970	3.946	3.908	3.812
	1.9	3.710	3.461	3.308	4.108	4.074	3.998
	2.1	3.754	3.541	3.424	4.161	4.127	4.108
	2.5	3.977	3.799	3.628	4.239	4.194	4.238
	3.0	4.184	4.008	3.868	4.248	4.212	4.337
	3.5	4.195	--	3.974	4.169	4.150	4.266
	4.0	4.294	4.193	4.093	4.140	4.126	4.241
	4.5	4.223	4.157	4.070	4.133	4.114	4.214
	5.0	4.276	4.194	4.098	4.162	4.136	4.243
	5.5	4.298	4.235	4.161	4.159	4.153	4.228

Approved for Public Release

Contrails

TABLE II

CONTINUED

	s, ins.	Run No. 25	26	27	28	29	30
p_{t_∞}, psia		449.3	599.2	607.0	600.7	598.2	598.8
M_∞		8.00	8.00	8.00	8.00	8.00	8.00
T_{t_∞}, °R		1279	1309	1314	1337	1324	1309
Re_∞/ft$\times 10^{-5}$		21.07	27.15	27.34	26.36	26.62	27.11
T_1, °R		530.1	129.3	146.6	149.5	155.7	161.4
T_2, °R		530.9	134.9	141.5	145.3	150.0	160.5
T_3, °R		531.6	137.5	146.4	152.8	162.2	163.5
p/p_∞	-3.5	.9825	.9161	.9447	.9415	.9479	.9441
	-3.0	.9805	.9174	.9572	.9553	.9577	.9389
	-2.5	.9727	.9254	.9620	.9687	.9663	.9452
	-2.3	.9861	.9144	.9687	.9847	.9616	.9697
	-2.1	.9854	.9420	.9864	.9642	.9548	.9598
	-1.9	--	.9799	.9932	.9618	.9503	.9612
	-1.7	.9867	.9444	.9624	.9855	.9637	.9706
	-1.5	.9972	.9567	.9686	.9909	.9779	.9679
	-1.3	1.047	.9233	.9885	.9848	.9853	.9717
	-1.1	1.155	.9451	.9761	.9923	.9872	.9683
	- .9	1.282	1.017	1.012	1.017	1.014	1.028
	- .7	1.397	1.223	1.106	1.196	1.218	1.275
	- .6	1.445	1.294	1.241	1.350	1.360	1.351
	- .5	1.491	1.362	1.369	1.458	1.448	1.422
	- .4	1.520	1.407	1.433	1.491	1.513	1.478
	- .3	1.550	1.437	1.478	1.547	1.546	1.491
	- .2	1.583	1.480	1.516	1.579	1.589	1.536
	- .1	1.593	1.496	1.549	1.608	1.615	1.561
	0.0	1.617	1.509	1.564	1.627	1.625	1.571
	.1	1.650	1.567	1.647	1.701	1.712	1.614
	.2	1.717	1.728	1.854	1.895	1.906	1.762
	.3	1.823	1.909	2.058	2.093	2.081	1.914
	.4	1.895	2.076	2.247	2.319	2.352	2.100
	.5	2.015	2.300	2.529	2.640	2.640	2.356
	.6	2.124	2.560	2.773	2.895	2.908	2.563
	.7	2.233	2.753	2.987	3.120	3.113	2.746
	.9	2.510	3.111	3.339	3.493	3.492	3.132
	1.1	2.630	3.328	3.614	3.728	3.762	3.279
	1.3	3.002	3.660	3.841	3.998	4.043	3.632
	1.5	3.332	3.767	3.890	4.156	4.162	3.799
	1.9	3.651	3.991	4.022	4.349	4.327	3.980
	2.1	3.776	4.075	4.048	4.409	4.407	4.025
	2.5	3.999	4.111	4.012	4.425	4.414	4.012
	3.0	4.172	4.092	4.109	4.441	4.418	4.071
	3.5	4.227	4.010	4.095	4.423	4.428	4.045
	4.0	4.266	4.081	4.106	4.404	4.402	4.046
	4.5	4.200	4.027	4.012	4.306	4.304	3.965
	5.0	4.220	4.047	4.054	4.387	4.370	4.019
	5.5	4.265	4.098	4.084	4.426	4.430	4.071

Approved for Public Release

Contrails

TABLE II

CONTINUED

	s, ins.	Run No. 31	32	33	34	35	36
p_{t_∞}, psia		598.7	598.4	605.7	604.0	599.0	601.4
M_∞		8.00	8.00	8.00	8.00	8.00	8.00
T_{t_∞}, ^oR		1310	1309	1310	1313	1273	1316
Re_∞/ft$\times 10^{-5}$		27.07	27.11	27.42	27.25	28.28	27.04
T_1, ^oR		168.5	172.8	182.2	186.5	189.9	215.2
T_2, ^oR		172.8	173.3	183.2	187.6	188.3	211.8
T_3, ^oR		173.8	173.9	187.0	193.1	189.2	217.5
p/p_∞	-3.5	.9281	.9471	.9337	.9550	.9331	.9534
	-3.0	.9263	.9546	.9452	.9654	.9539	.9546
	-2.5	.9284	.9491	.9536	.9532	.9560	.9629
	-2.3	.9415	.9577	.9513	.9795	.9596	.9694
	-2.1	.9585	.9678	.9701	.9514	.9492	1.019
	-1.9	.9414	.9649	.9698	.9584	.9538	.9678
	-1.7	.9513	.9761	.9752	.9735	.9819	.9827
	-1.5	.9575	.9701	.9879	.9817	.9807	.9921
	-1.3	.9444	.9746	.9666	.9737	.9644	.9784
	-1.1	.9579	.9743	.9841	.9781	.9956	.9941
	- .9	1.069	1.029	1.106	1.098	1.116	1.159
	- .7	1.269	1.256	1.354	1.345	1.345	1.383
	- .6	1.344	1.354	1.434	1.415	1.437	1.435
	- .5	1.395	1.424	1.491	1.479	1.484	1.486
	- .4	1.435	1.465	1.519	1.511	1.517	1.550
	- .3	1.467	1.489	1.560	1.558	1.553	1.572
	- .2	1.500	1.526	1.594	1.592	1.581	1.605
	- .1	1.527	1.561	1.592	1.617	1.621	1.631
	0.0	1.535	1.566	1.613	1.629	1.611	1.637
	.1	1.593	1.636	1.659	1.678	1.670	1.694
	.2	1.733	1.747	1.799	1.838	1.811	1.812
	.3	1.885	1.936	1.997	2.007	1.979	1.952
	.4	2.041	2.155	2.172	2.180	2.208	2.149
	.5	2.267	2.370	2.428	2.417	2.471	2.372
	.6	2.470	2.576	2.609	2.735	2.671	2.558
	.7	2.662	2.775	2.863	2.931	2.874	2.763
	.9	3.034	3.157	3.255	3.319	3.267	3.162
	1.1	3.229	3.272	3.442	3.758	3.395	3.425
	1.3	3.593	3.616	3.796	4.027	3.772	3.788
	1.5	3.759	3.804	4.046	4.088	4.048	3.993
	1.9	3.964	3.951	4.282	4.300	4.299	4.277
	2.1	4.031	4.002	4.376	4.373	4.371	4.358
	2.5	4.079	4.006	4.435	4.419	4.432	4.421
	3.0	4.145	4.057	4.526	4.484	4.493	4.530
	3.5	4.054	4.012	4.442	4.429	4.441	4.450
	4.0	4.076	4.008	4.416	4.406	4.420	4.420
	4.5	3.970	3.923	4.311	4.306	4.329	4.321
	5.0	4.006	4.000	4.364	4.348	4.413	4.370
	5.5	4.057	4.051	4.390	4.415	4.429	4.416

Approved for Public Release

Contrails

TABLE II

CONTINUED

	s, ins.	Run No. 37	38	39	40	41	42
pt_∞, psia		602.3	600.8	598.1	601.0	599.8	599.1
M_∞		8.00	8.00	8.00	8.00	8.00	8.00
Tt_∞, °R		1312	1314	1319	1315	1304	1310
Re_∞/ft x 10^{-5}		27.18	27.07	26.77	27.03	27.33	27.10
T_1, °R		221.6	233.9	238.7	244.2	252.6	267.2
T_2, °R		216.9	232.0	236.0	245.8	252.3	263.9
T_3, °R		213.0	231.4	233.8	253.1	255.9	261.6
p/p_∞	-3.5	.9521	.9475	.9215	.9353	.9379	.9453
	-3.0	.9651	.9537	.9461	.9464	.9362	.9538
	-2.5	.9653	.9580	.9445	.9491	.9428	.9511
	-2.3	.9789	.9531	.9318	.9538	.9512	.9530
	-2.1	.9934	.9863	.9567	.9608	.9507	.9678
	-1.9	.9675	.9720	.9456	.9645	.9452	.9559
	-1.7	.9884	.9882	.9570	.9455	.9592	.9751
	-1.5	.9851	1.001	.9643	.9485	.9726	.9858
	-1.3	.9932	.9745	.9880	.9574	.9597	.9805
	-1.1	.9979	1.038	1.059	.9878	.9914	1.055
	- .9	1.106	1.210	1.212	1.116	1.151	1.266
	- .7	1.345	1.394	1.372	1.310	1.323	1.419
	- .6	1.414	1.453	1.418	1.374	1.381	1.470
	- .5	1.492	1.515	1.466	1.425	1.431	1.517
	- .4	1.512	1.541	1.504	1.457	1.459	1.557
	- .3	1.567	1.564	1.517	1.496	1.493	1.571
	- .2	1.597	1.606	1.538	1.535	1.536	1.598
	- .1	1.614	1.621	1.568	1.561	1.557	1.629
	0.0	1.643	1.633	1.563	1.584	1.567	1.630
	.1	1.689	1.678	1.596	1.621	1.600	1.665
	.2	1.836	1.790	1.674	1.758	1.705	1.755
	.3	1.993	1.939	1.792	1.900	1.849	1.891
	.4	2.174	2.121	1.957	2.055	1.978	2.051
	.5	2.400	--	2.135	2.262	2.177	2.256
	.6	2.657	2.559	2.237	2.487	2.388	2.416
	.7	2.863	2.722	2.440	2.685	2.560	2.597
	.9	3.241	3.134	2.800	3.067	2.949	2.973
	1.1	3.506	3.297	3.066	3.403	3.145	3.157
	1.3	3.841	3.681	3.435	3.686	3.530	3.576
	1.5	4.047	3.984	3.613	3.792	3.747	3.873
	1.9	4.292	4.253	3.886	3.954	3.963	4.203
	2.1	4.365	4.344	3.956	4.059	4.039	4.308
	2.5	4.439	4.430	4.055	4.103	4.117	4.402
	3.0	4.496	4.531	4.204	4.257	4.194	4.541
	3.5	4.440	4.472	4.179	4.111	4.101	4.491
	4.0	4.411	4.434	4.127	4.120	4.121	4.439
	4.5	4.319	4.334	4.104	4.064	4.035	4.330
	5.0	4.373	4.389	4.109	4.105	4.112	4.378
	5.5	4.401	4.394	4.116	4.148	4.136	4.385

Approved for Public Release

Contrails

TABLE II

CONTINUED

	s, ins.	Run No. 43	44	45	46	47	48
p_{t_∞}, psia		603.1	603.7	603.2	603.7	597.2	595.8
M_∞		8.00	8.00	8.00	8.00	8.00	8.00
T_{t_∞}, °R		1314	1313	1314	1304	1315	1312
Re_∞/ft$\times 10^{-5}$		27.15	27.23	27.15	27.50	26.85	26.89
T_1, °R		297.6	308.4	350.1	368.0	523.9	526.8
T_2, °R		302.8	313.2	352.6	370.0	523.7	527.3
T_3, °R		305.1	314.7	357.3	369.6	524.4	528.1
p/p_∞	-3.5	.9344	.9661	.9303	.9390	.9486	.9564
	-3.0	.9449	.9349	.9419	.9639	.9545	.9588
	-2.5	.9487	.9524	.9441	.9491	.9595	.9682
	-2.3	.9237	.9288	.9503	.9541	.9637	.9754
	-2.1	.9479	.9549	.9504	.9669	.9565	.9719
	-1.9	.9301	.9378	.9776	.9673	.9897	1.003
	-1.7	.9397	.9535	.9573	.9687	.9701	.9807
	-1.5	.9560	.9749	.9442	.9821	1.008	1.015
	-1.3	.9859	.9839	.9928	.9954	1.115	1.119
	-1.1	1.100	1.116	1.091	1.133	1.258	1.262
	- .9	1.271	1.268	1.267	1.243	1.340	1.361
	- .7	1.389	1.399	1.375	1.376	1.420	1.435
	- .6	1.445	1.433	1.425	1.416	1.452	1.461
	- .5	1.478	1.466	1.462	1.459	1.489	1.495
	- .4	1.482	1.502	1.478	1.482	1.492	1.511
	- .3	1.521	1.517	1.516	1.501	1.522	1.527
	- .2	1.540	1.543	1.543	1.528	1.545	1.549
	- .1	1.546	1.552	1.557	1.562	1.560	1.575
	0.0	1.569	1.574	1.572	1.580	1.570	1.580
	.1	1.595	1.598	1.605	1.607	1.593	1.607
	.2	1.670	1.646	1.687	1.668	1.650	1.656
	.3	1.769	1.758	1.789	1.791	1.731	1.728
	.4	1.868	1.898	1.897	1.877	1.802	1.809
	.5	2.013	2.053	2.079	2.037	1.920	1.935
	.6	2.241	2.222	2.224	2.183	2.039	2.026
	.7	2.427	2.391	2.394	2.342	2.168	2.164
	.9	2.811	2.759	2.751	2.668	2.444	2.442
	1.1	3.110	3.036	3.154	2.888	2.746	2.628
	1.3	3.471	3.419	3.474	3.293	3.100	3.007
	1.5	3.652	3.622	3.594	3.500	3.317	3.310
	1.9	3.910	3.901	3.869	3.836	3.662	3.656
	2.1	3.964	3.957	3.949	3.919	3.771	3.787
	2.5	4.118	4.099	4.040	3.995	3.956	3.953
	3.0	4.223	4.237	4.262	4.123	4.203	4.207
	3.5	4.207	4.200	4.188	4.177	4.189	4.208
	4.0	4.144	4.149	4.161	4.152	4.254	4.266
	4.5	4.048	4.048	4.077	4.050	4.158	4.168
	5.0	4.119	4.115	4.122	4.091	4.156	4.165
	5.5	4.114	4.113	4.156	4.135	4.192	4.205

Approved for Public Release

Contrails

TABLE II

CONTINUED

	s, ins.	Run No. 49	50	51	52	53	54
p_{t_∞}, psia		603.1	602.3	600.3	603.8	598.7	598.0
M_∞		8.00	8.00	8.00	8.00	8.00	8.00
T_{t_∞}, °R		1310	1331	1321	1337	1306	1305
$Re_\infty/ft \times 10^{-5}$		27.30	26.62	26.81	26.49	27.20	27.20
T_1, °R		530.3	547.9	542.9	554.8	545.4	549.2
T_2, °R		528.2	545.6	542.5	554.5	547.6	551.1
T_3, °R		527.4	546.0	542.8	555.5	550.1	553.4
p/p_∞	-3.5	.9346	.9535	.9425	.9578	.9426	.9319
	-3.0	.9472	.9565	.9442	.9602	.9476	.9386
	-2.5	.9442	.9627	.9520	.9611	.9568	.9455
	-2.3	.9610	.9693	.9610	.9720	.9664	.9462
	-2.1	.9507	1.006	.9585	.9982	.9636	.9540
	-1.9	.9503	.9769	1.002	.9650	.9681	.9632
	-1.7	.9741	.9949	.9713	1.005	.9834	.9765
	-1.5	1.019	1.076	1.011	1.074	1.036	1.034
	-1.3	1.120	1.164	1.110	1.163	1.142	1.161
	-1.1	1.248	1.298	1.253	1.306	1.273	1.254
	- .9	1.348	1.390	1.343	1.391	1.355	1.377
	- .7	1.412	1.466	1.420	1.463	1.428	1.421
	- .6	1.440	1.500	1.462	1.502	1.458	1.458
	- .5	1.475	1.528	1.482	1.530	1.482	1.481
	- .4	1.486	1.554	1.508	1.523	1.524	1.501
	- .3	1.509	1.565	1.516	1.563	1.520	1.516
	- .2	1.535	1.587	1.547	1.583	1.540	1.544
	- .1	1.555	1.609	1.564	1.594	1.575	1.562
	0.0	1.558	1.607	1.576	1.607	1.574	1.568
	.1	1.575	1.644	1.603	1.626	1.599	1.593
	.2	1.634	1.684	1.649	1.664	1.645	1.643
	.3	1.694	1.781	1.730	1.724	1.706	1.678
	.4	1.771	1.835	1.803	1.801	1.797	1.752
	.5	1.883	1.946	1.927	1.899	1.903	1.858
	.6	2.008	2.029	2.026	2.037	1.998	1.984
	.7	2.125	2.140	2.161	2.147	2.112	2.085
	.9	2.392	2.428	2.432	2.440	2.365	2.348
	1.1	2.589	2.519	2.582	2.577	2.571	2.618
	1.3	2.974	2.939	2.968	2.972	2.956	2.998
	1.5	3.247	3.328	3.285	3.321	3.224	3.200
	1.9	3.628	3.721	3.653	3.733	3.618	3.608
	2.1	3.775	3.854	3.744	3.850	3.761	3.748
	2.5	3.923	4.094	3.932	4.094	3.902	3.889
	3.0	4.116	4.272	4.140	4.250	4.116	4.109
	3.5	4.192	4.300	4.187	4.283	4.175	4.165
	4.0	4.252	4.393	4.236	4.343	4.234	4.224
	4.5	4.146	4.326	4.138	4.293	4.153	4.129
	5.0	4.154	4.319	4.149	4.290	4.149	4.125
	5.5	4.172	4.334	4.206	4.307	4.164	4.158

Approved for Public Release

Contrails

TABLE II

CONCLUDED

	s, ins.	Run No. 55	Run No. 56
Pt_∞, psia		148.8	449.5
M_∞		7.96	8.00
T_{t_∞}, °R		1200	1277
Re_∞/ft×10^{-5}		7.781	21.12
T_1, °R		532.1	359.7
T_2 °R		531.9	361.1
T_3		531.9	365.6
p/p_∞	-3.5	1.051	.9668
	-3.0	1.039	.9733
	-2.5	1.047	.9765
	-2.3	1.019	.9849
	-2.1	1.007	.9683
	-1.9	1.027	--
	-1.7	1.040	.9795
	-1.5	1.023	.9816
	-1.3	1.047	1.001
	-1.1	1.065	1.037
	- .9	1.051	1.149
	- .7	1.078	1.313
	- .6	1.161	1.394
	- .5	1.231	1.454
	- .4	1.296	1.496
	- .3	1.375	1.537
	- .2	1.431	1.577
	- .1	1.500	1.609
	0.0	1.574	1.615
	.1	1.654	1.673
	.2	1.722	1.770
	.3	1.883	1.922
	.4	1.909	2.009
	.5	1.987	2.176
	.6	2.126	2.325
	.7	2.192	2.490
	.9	2.416	2.840
	1.1	2.650	2.997
	1.3	2.899	3.367
	1.5	3.122	3.667
	1.9	3.380	3.923
	2.1	3.564	4.004
	2.5	3.784	4.158
	3.0	3.948	4.341
	3.5	4.151	4.295
	4.0	4.272	4.271
	4.5	4.265	4.225
	5.0	4.364	4.242
	5.5	4.415	4.260

Approved for Public Release

TABLE III

THEORETICAL DISTANCE BETWEEN INFLECTION POINT AND SEPARATION POINT FOR A RANGE OF INITIAL QUANTITIES

Run No.	Initial Conditions						x_i [1]	$x_s - x_i$ [2]	x_s
	p_{t_∞}	M_o	Re_o/ft	T_w/T_{t_∞}	L'_E (ft)	L (ft)	(ft)	(ft)	(ft)
1	150	6.72	0.48^6	0.221	0.582	0.761	(3)	0.0076	--
3	150	6.72	$.48^6$	.293	.508	.737	(3)	.0090	--
55	150	6.72	$.48^6$	.443	.330	.722	(3)	.0115	--
13	300	6.76	$.82^6$	.212	.617	.747	0.776	.0068	0.783
14	300	6.76	$.82^6$	.265	.584	.720	.770	.0083	.778
16	300	6.76	$.82^6$	.296	.526	.710	.767	.0086	.776
17	300	6.76	$.82^6$	.428	.375	.697	.755	.0109	.766
24	450	6.81	1.15^6	.206	.775	.715	.756	.0074	.763
56	450	6.81	1.15^6	.284	.667	.687	.750	.0095	.760
25	450	6.81	1.15^6	.415	.460	.661	.731	.0113	.742
42	600	6.83	1.48^6	.202	.833	.705	.738	.0065	.744
44	600	6.83	1.48^6	.238	.791	.681	.735	.0077	.743
46	600	6.83	1.48^6	.283	.737	.674	.737	.0099	.747
48	600	6.83	1.48^6	.402	.564	.638	.717	.0121	.729

[1]Experimental values.

[2]Theoretical values.

[3]Inflection point indistinguishable in experimental pressure distribution.

Approved for Public Release

Confidential

Contrails

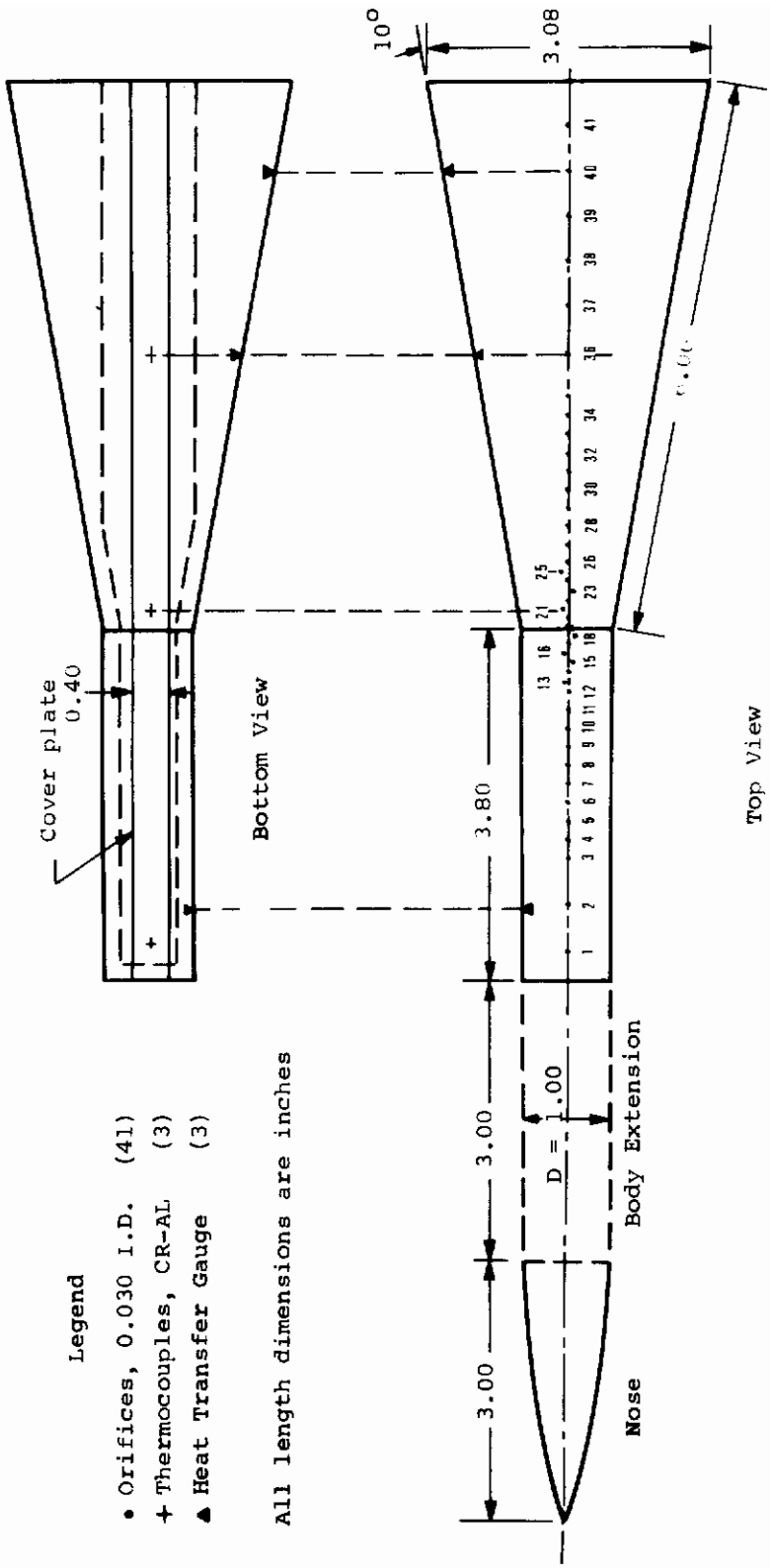

Figure 1.- Wind-tunnel model to study effect of cooling on extent of laminar separation.

Approved for Public Release

Contrails

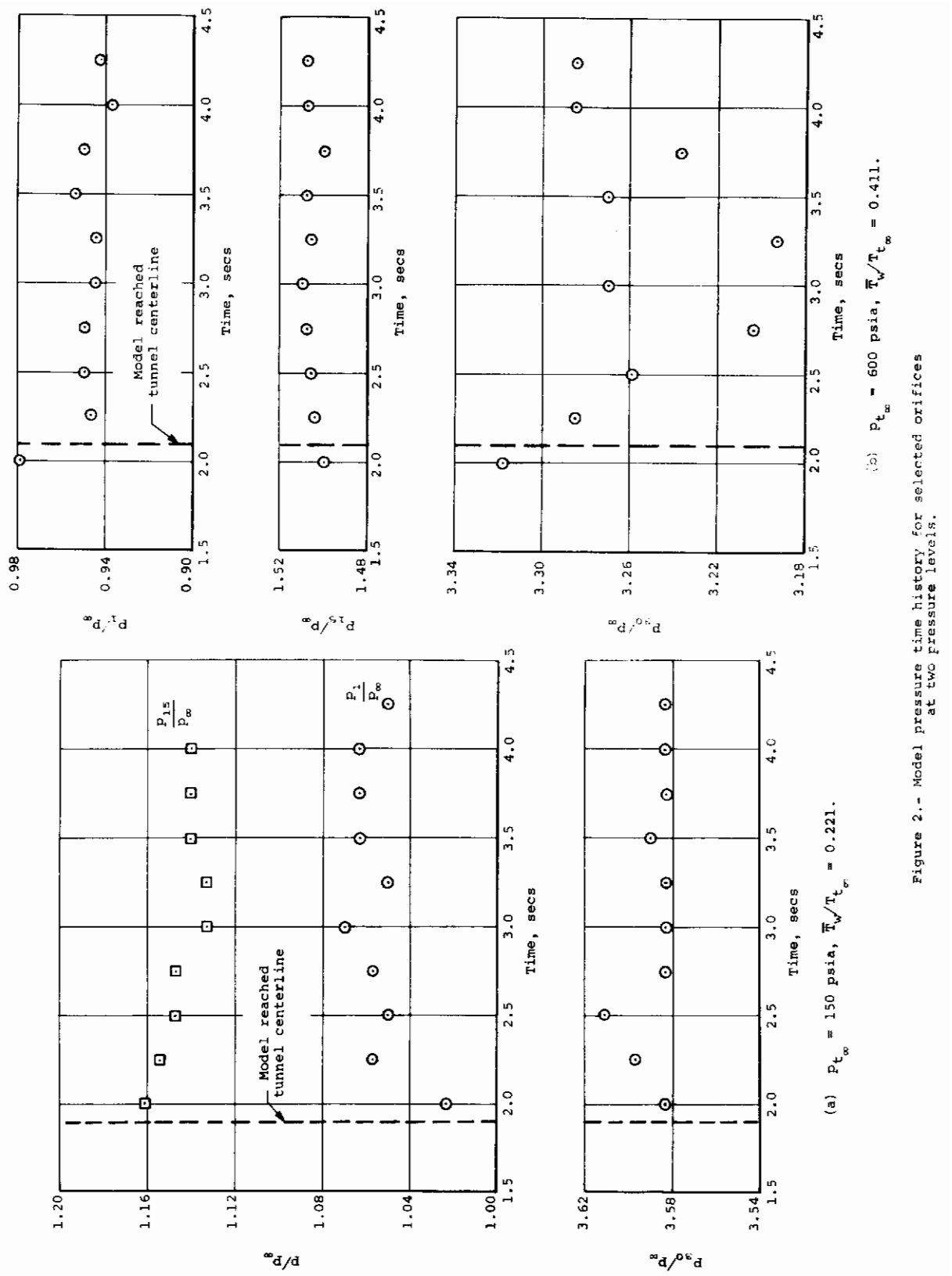

Figure 2.- Model pressure time history for selected orifices at two pressure levels.

(a) p_{t_∞} = 150 psia, $\bar{T}_w/T_{t_\infty}$ = 0.221.

(b) p_{t_∞} = 600 psia, $\bar{T}_w/T_{t_\infty}$ = 0.411.

Approved for Public Release

Contrails

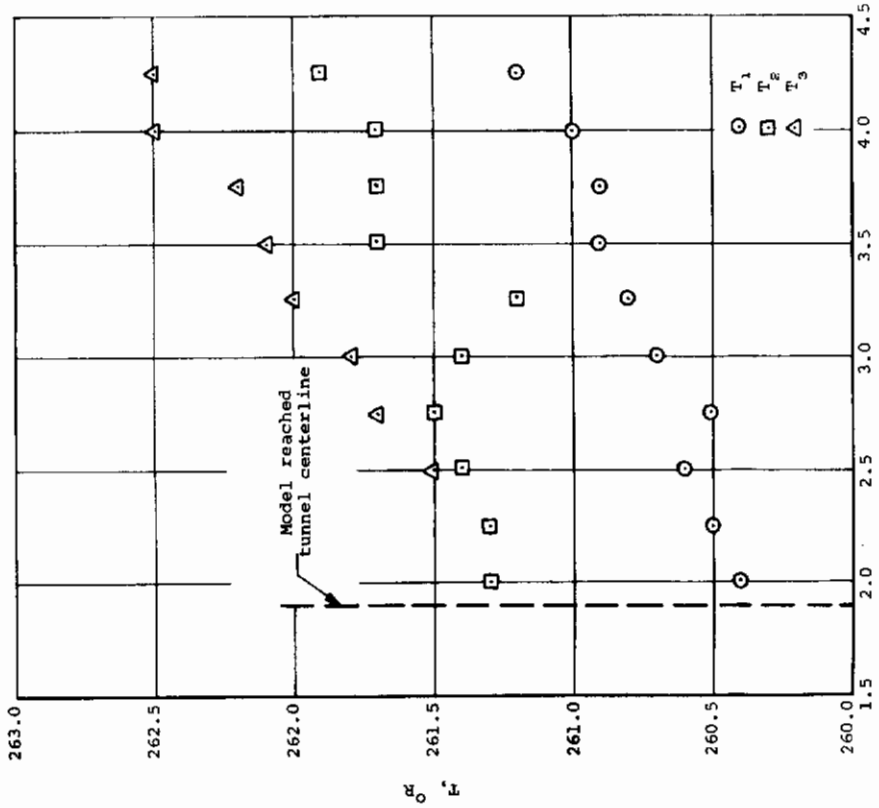

(a) P_{t_∞} = 150 psia, $\overline{T}_w/T_{t_\infty}$ = 0.221.

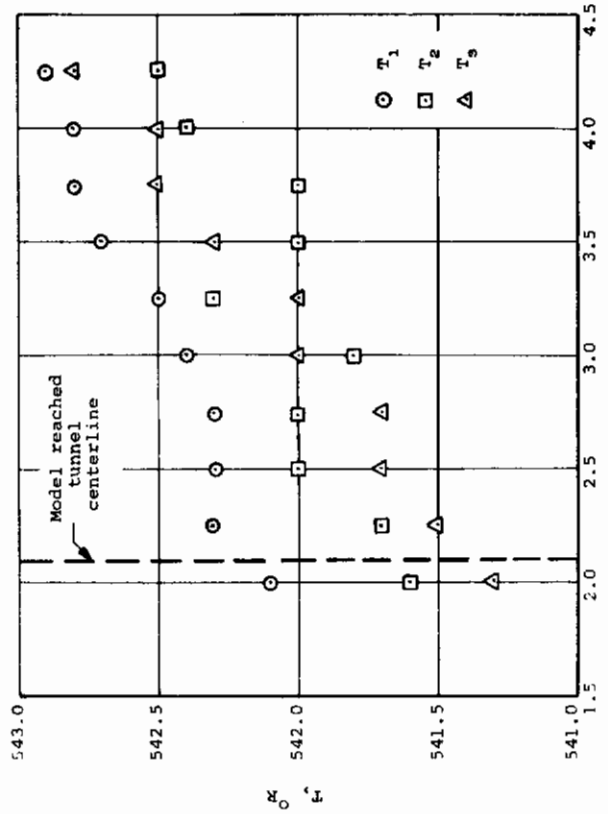

(b) P_{t_∞} = 600 psia, $\overline{T}_w/T_{t_\infty}$ = 0.411.

Figure 3.- Model temperature time history for two pressure levels.

Approved for Public Release

Contrails

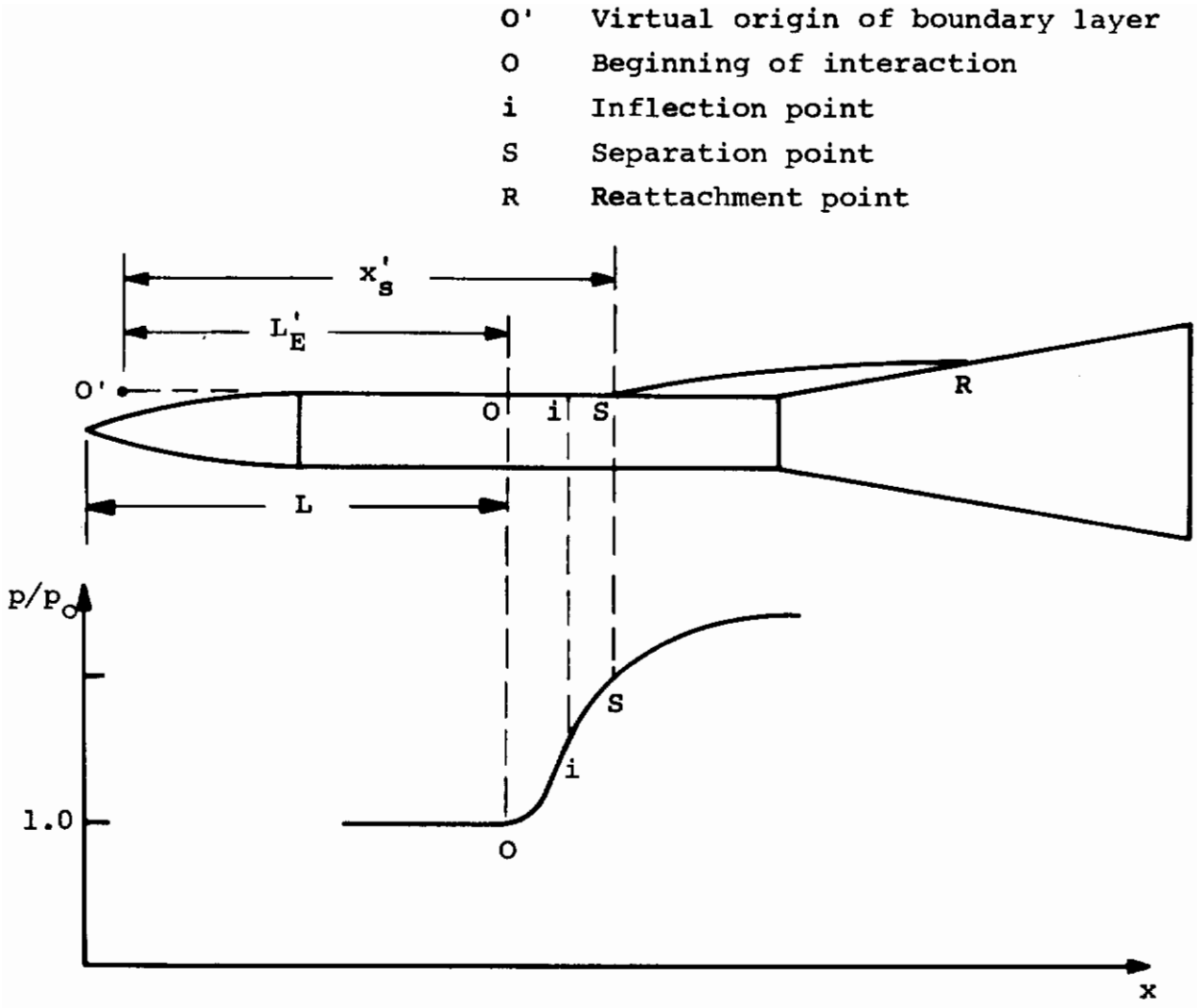

Figure 4.- Separated flow details and pressure distribution for ogive-cylinder-flare combination.

Approved for Public Release

Contrails

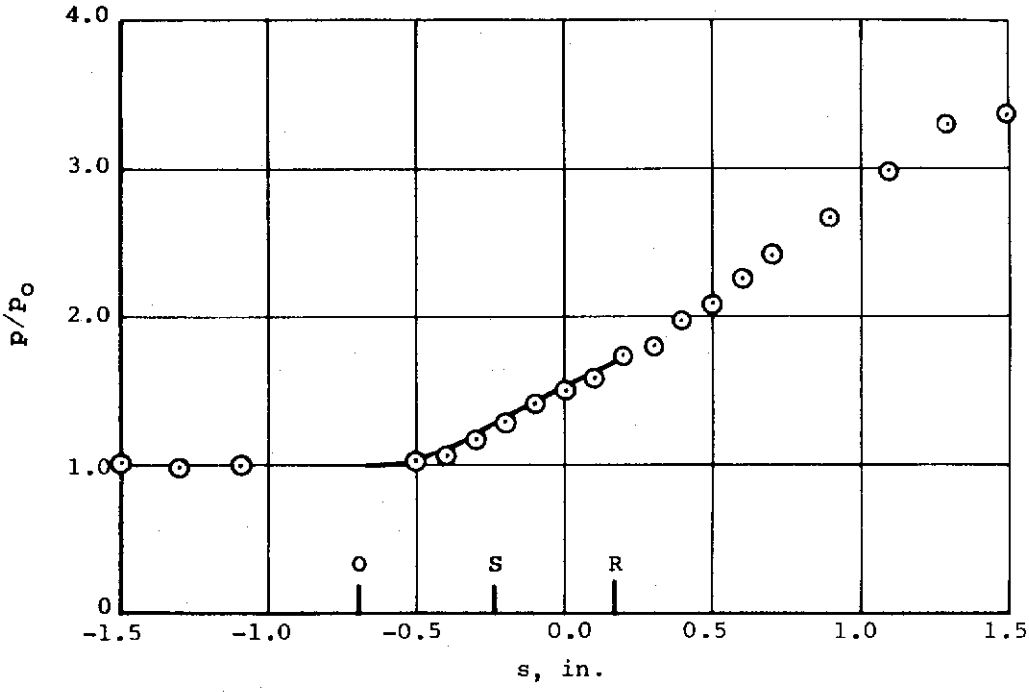

(a) p_{t_∞} = 150 psia, $\overline{T}_w/T_{t_\infty}$ = 0.221.

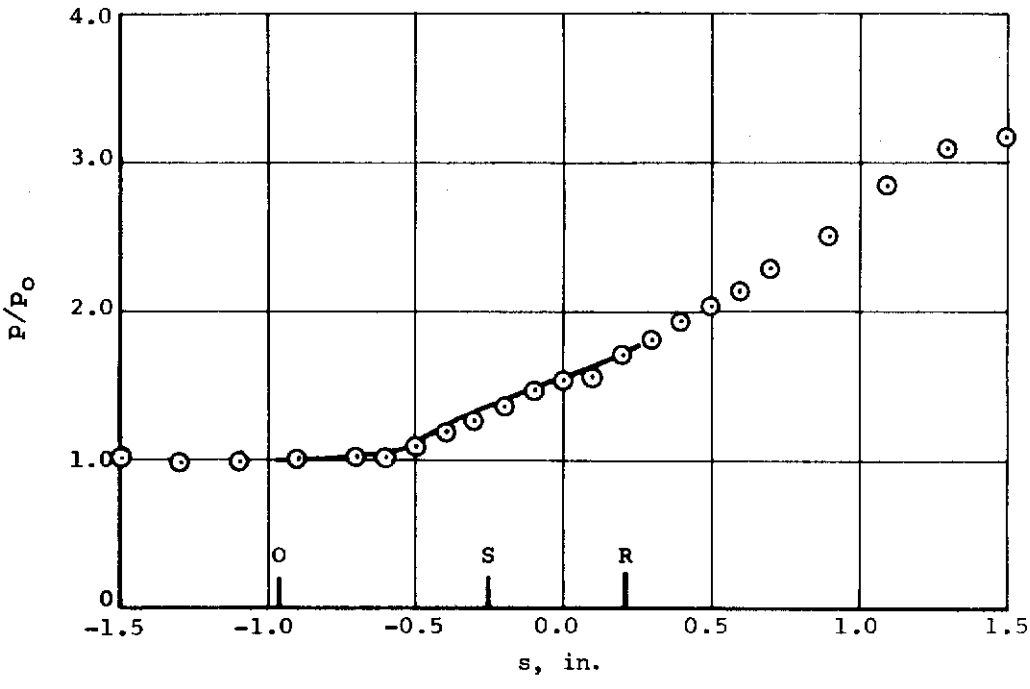

(b) p_{t_∞} = 150 psia, $\overline{T}_w/T_{t_\infty}$ = 0.293.

Figure 5.- Comparison between experimental pressure distributions and theoretically fitted pressure distributions.

Approved for Public Release

Contrails

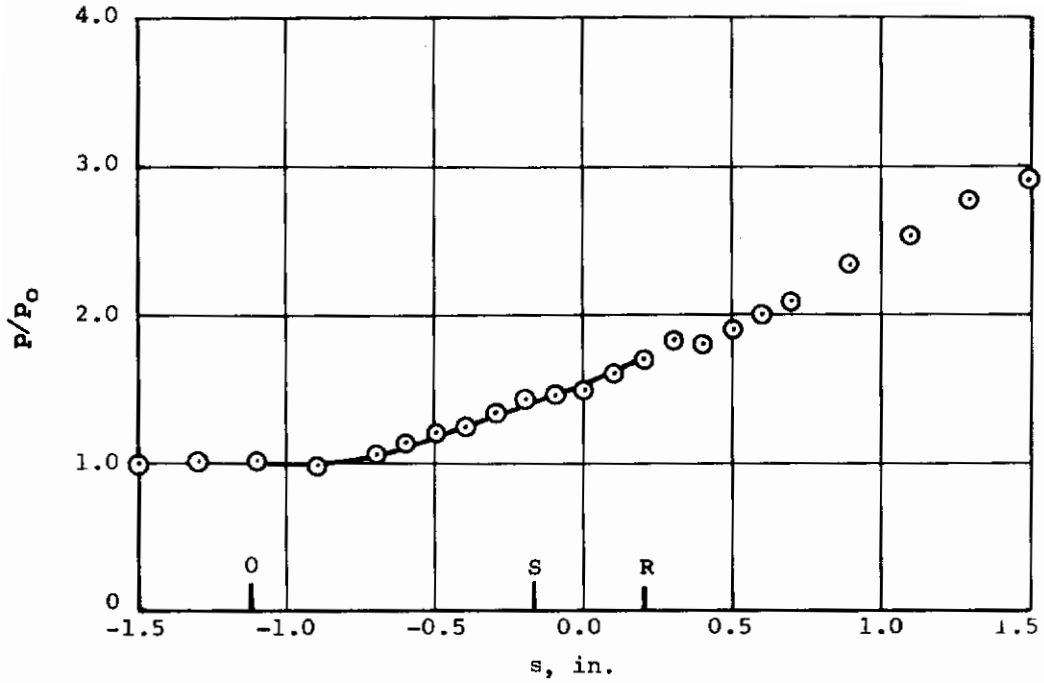

(c) p_{t_∞} = 150 psia, $\overline{T}_w/T_{t_\infty}$ = 0.443.

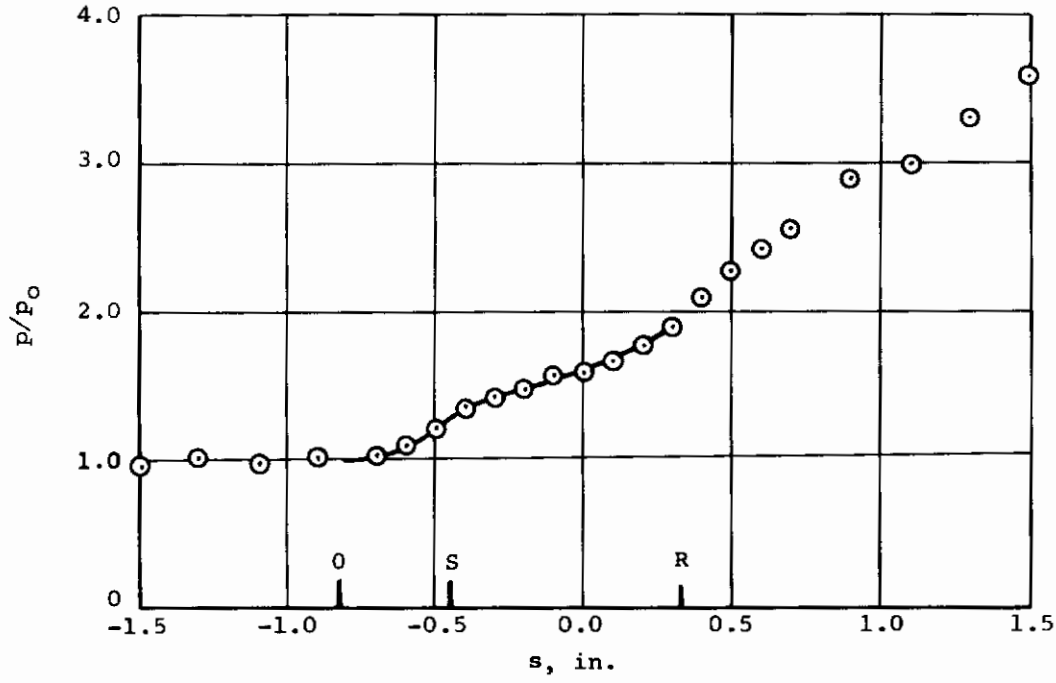

(d) p_{t_∞} = 300 psia, $\overline{T}_w/T_{t_\infty}$ = 0.212.

Figure 5.- Continued.

Approved for Public Release

Contrails

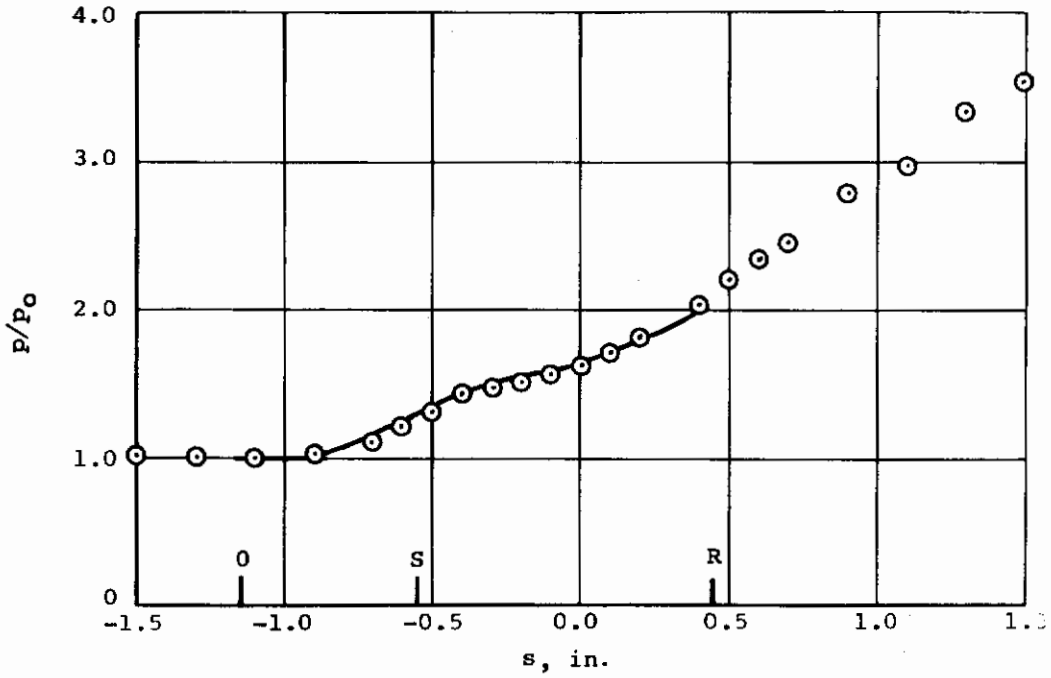

(e) p_{t_∞} = 300 psia, $\overline{T}_w/T_{t_\infty}$ = 0.265.

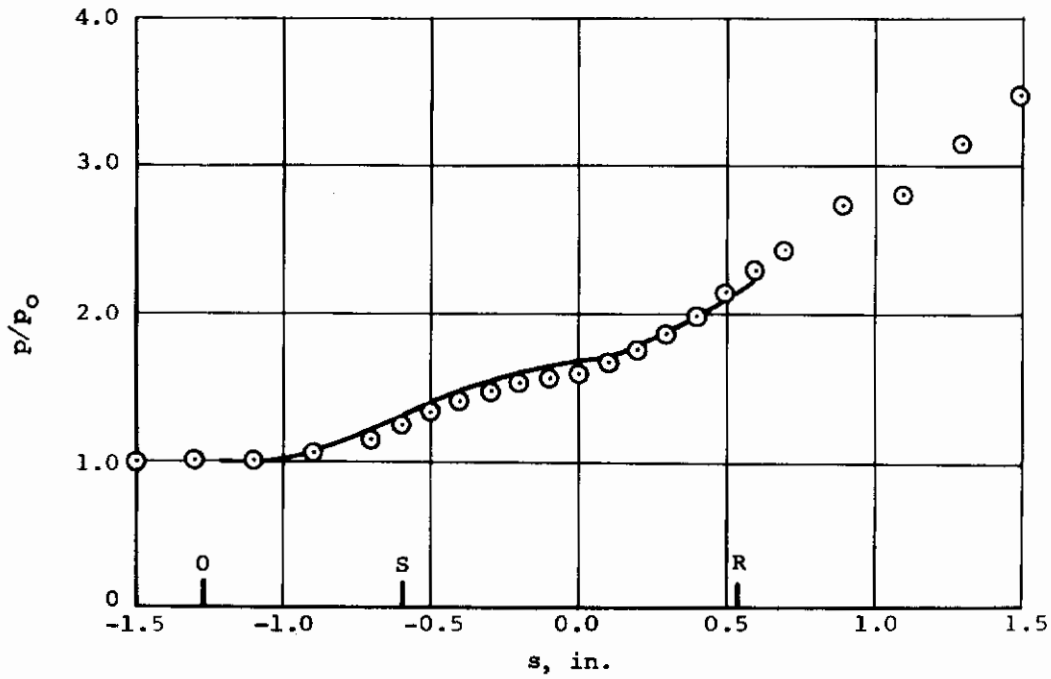

(f) p_{t_∞} = 300 psia, $\overline{T}_w/T_{t_\infty}$ = 0.296.

Figure 5.- Continued.

Approved for Public Release

Contrails

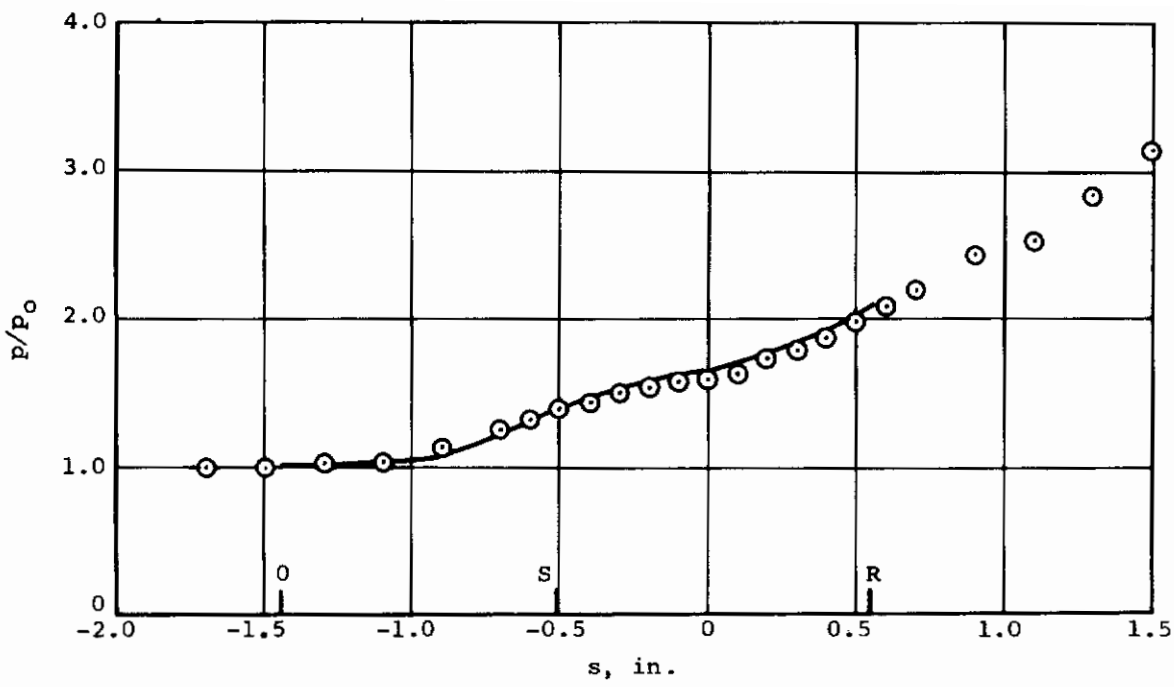

(g) p_{t_∞} = 300 psia, $\overline{T}_w/T_{t_\infty}$ = 0.428.

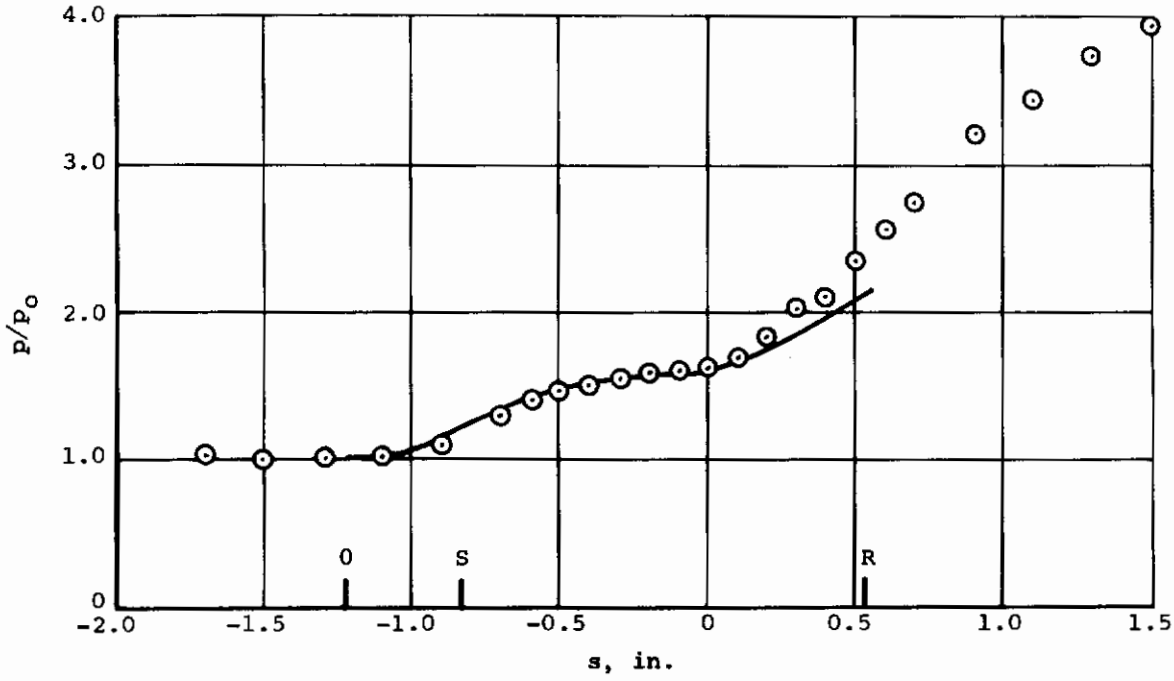

(h) p_{t_∞} = 450 psia, $\overline{T}_w/T_{t_\infty}$ = 0.206.

Figure 5.- Continued.

Approved for Public Release

Contrails

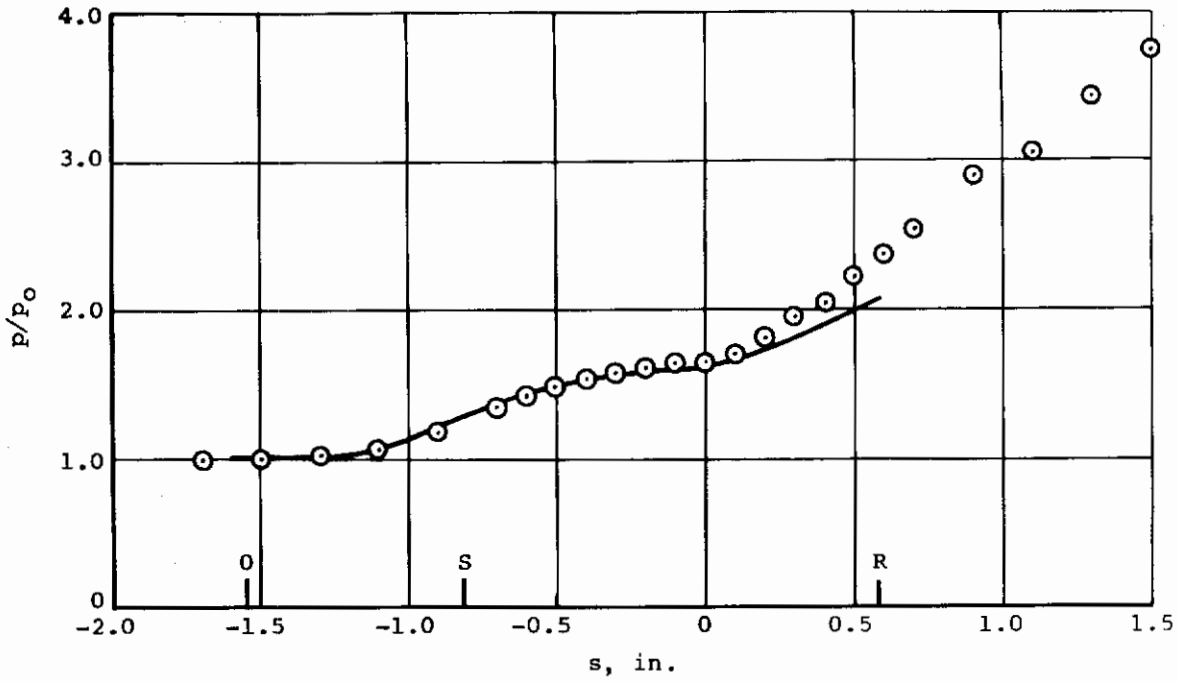

(i) p_{t_∞} = 450 psia, $\overline{T}_w/T_{t_\infty}$ = 0.284.

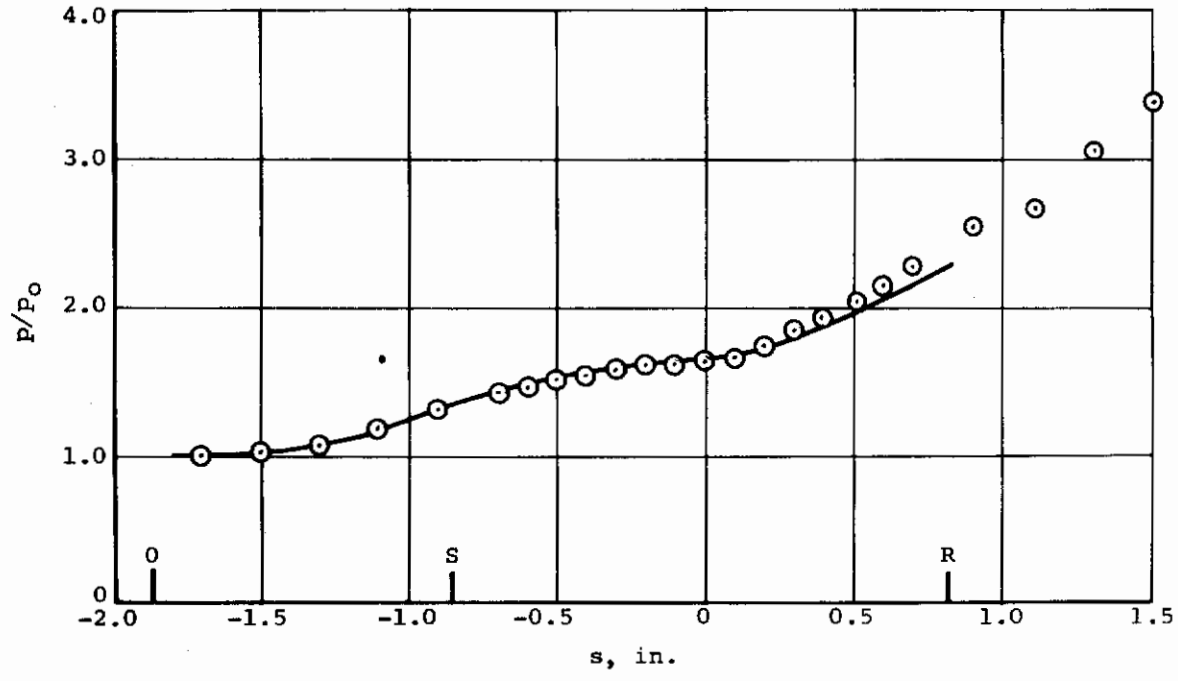

(j) p_{t_∞} = 450 psia, $\overline{T}_w/T_{t_\infty}$ = 0.415.

Figure 5.- Continued.

Approved for Public Release

Contrails

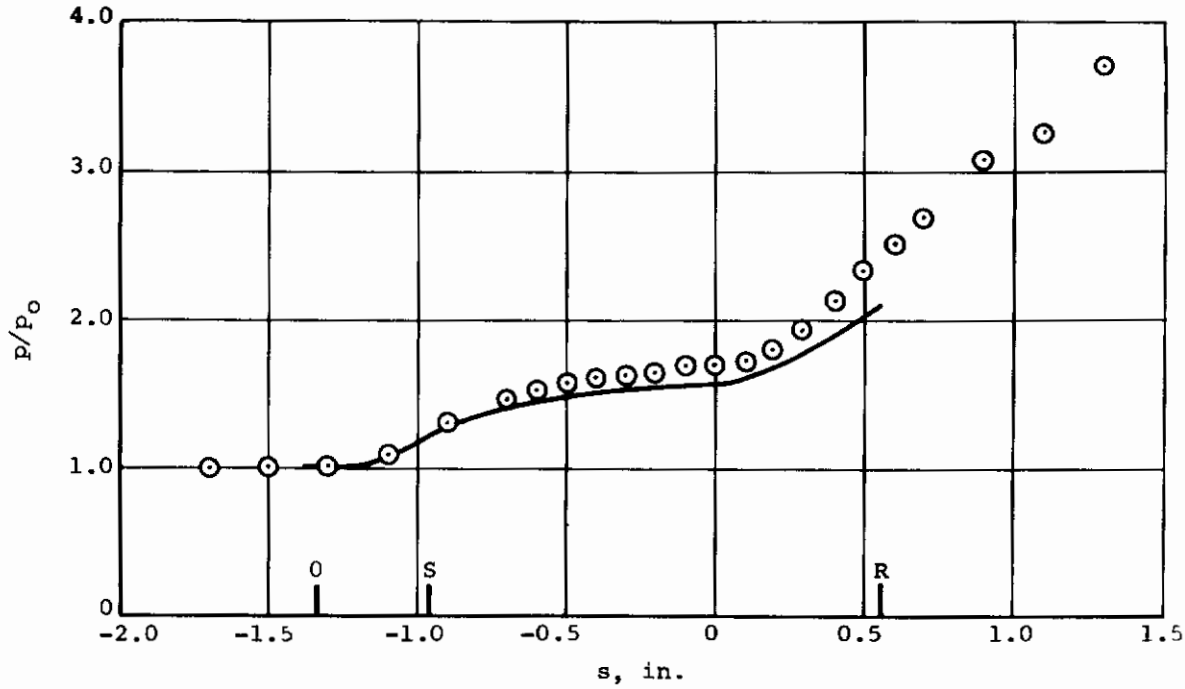

(k) p_{t_∞} = 600 psia, $\overline{T}_w/T_{t_\infty}$ = 0.202.

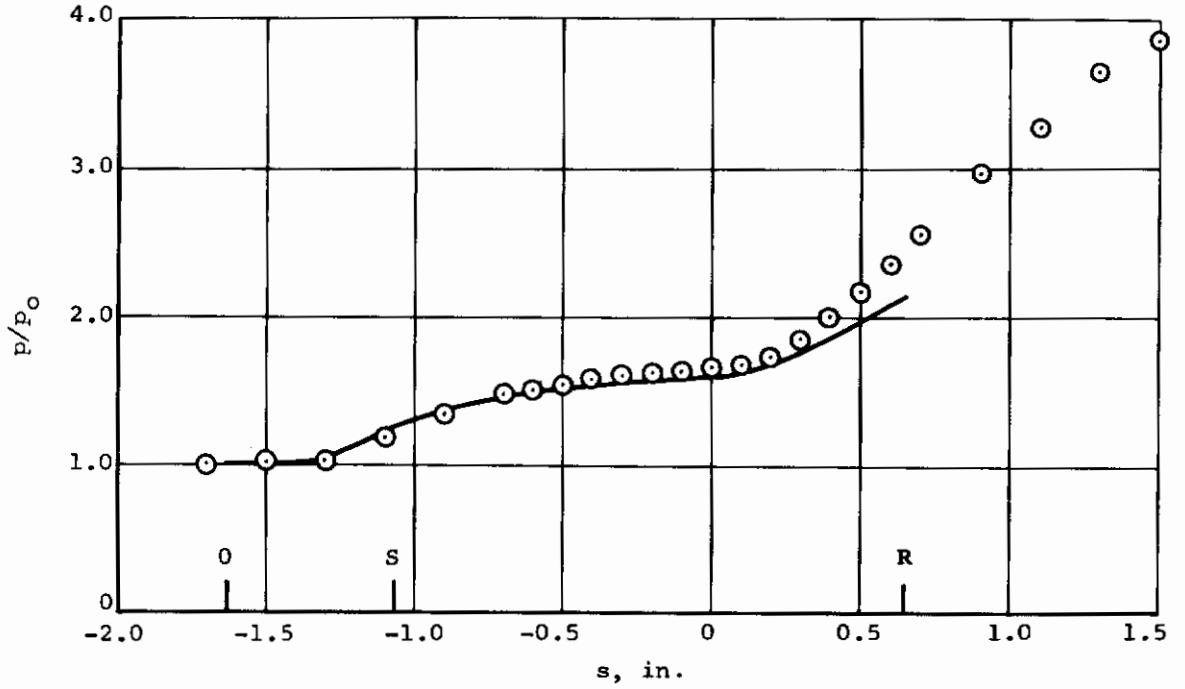

(l) p_{t_∞} = 600 psia, $\overline{T}_w/T_{t_\infty}$ = 0.238.

Figure 5.- Continued.

Approved for Public Release

Contrails

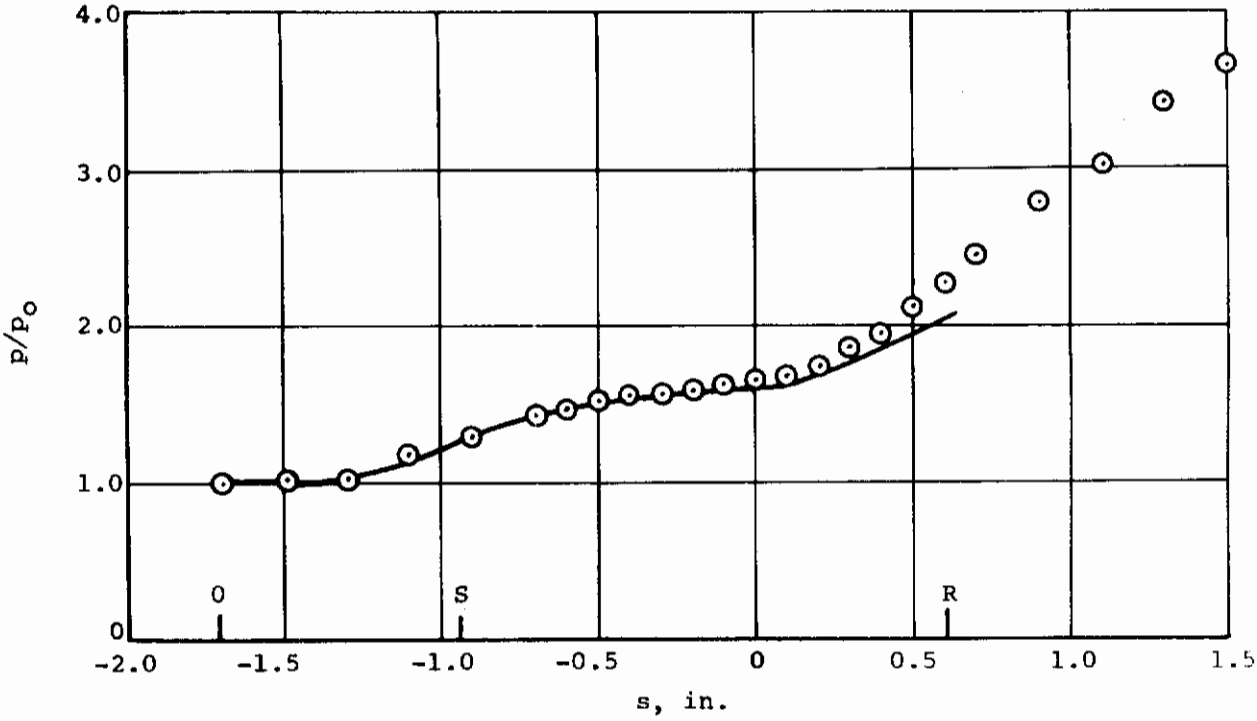

(m) p_{t_∞} = 600 psia, $\overline{T}_w/T_{t_\infty}$ = 0.283.

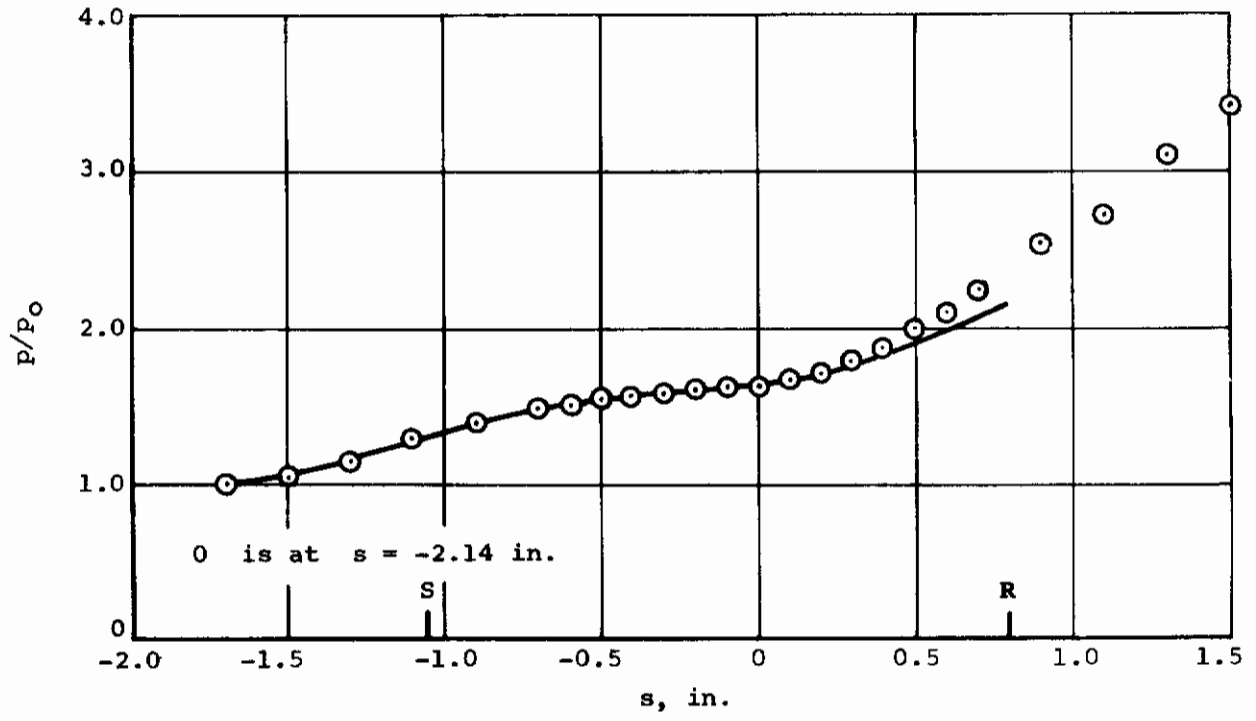

(n) p_{t_∞} = 600 psia, $\overline{T}_w/T_{t_\infty}$ = 0.402.

Figure 5.- Concluded.

Approved for Public Release

Contrails

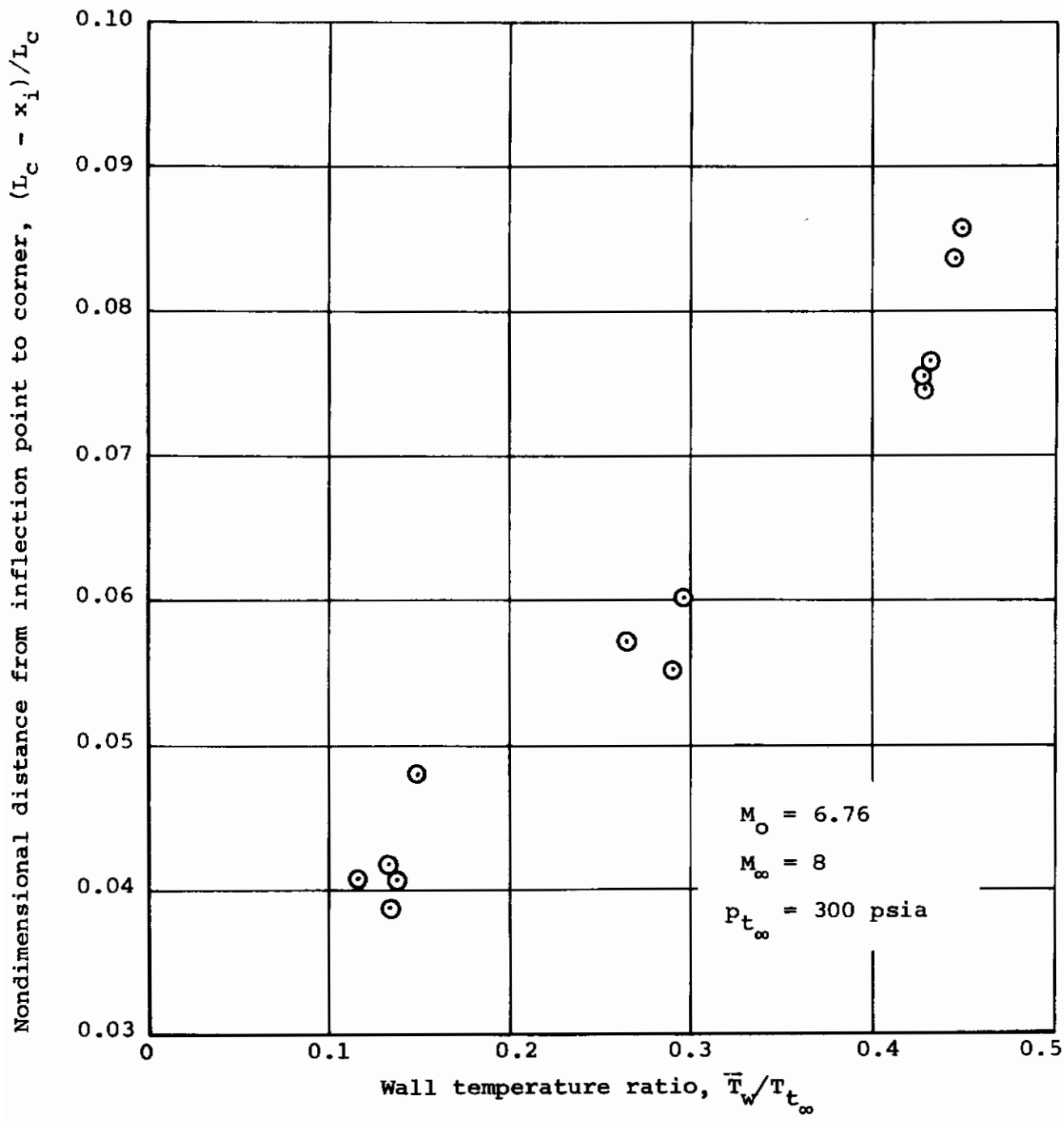

(a) p_{t_∞} = 300 psia.

Figure 6.- Effect of wall temperature ratio on distance between inflection point and corner; prime data.

Approved for Public Release

Contrails

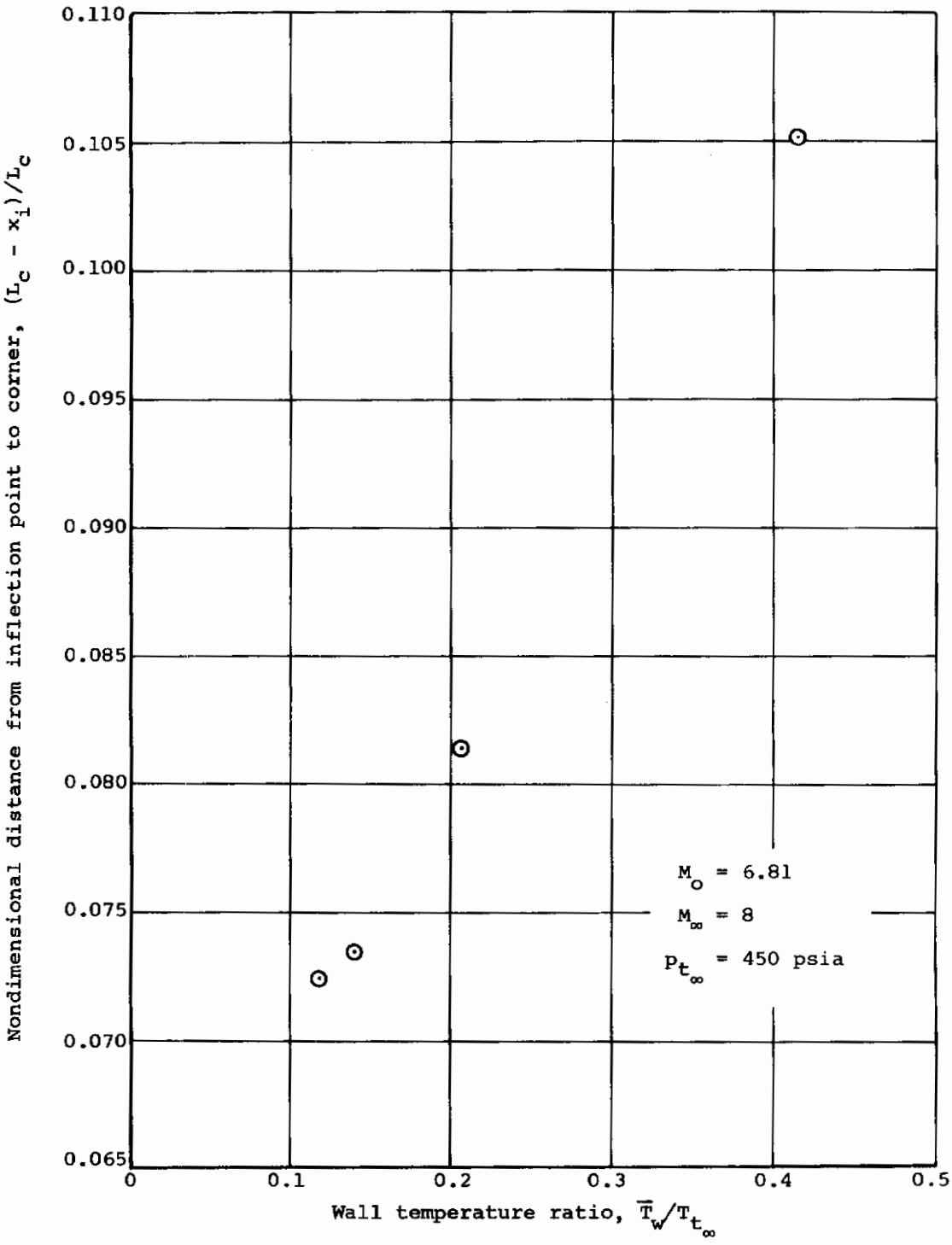

(b) p_{t_∞} = 450 psia.

Figure 6.- Continued.

Approved for Public Release

Contrails

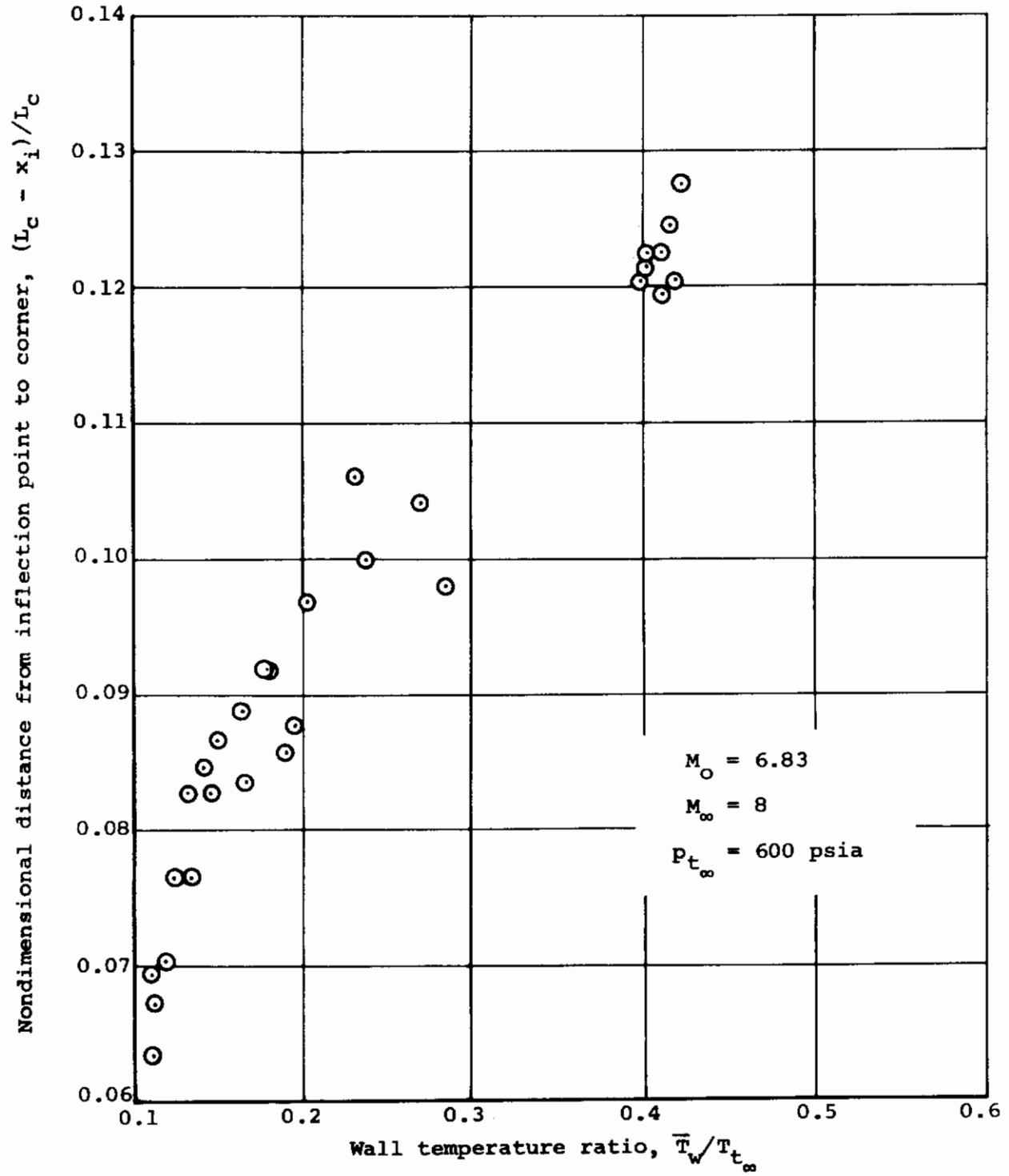

(c) p_{t_∞} = 600 psia.

Figure 6.- Concluded.

Approved for Public Release

Contrails

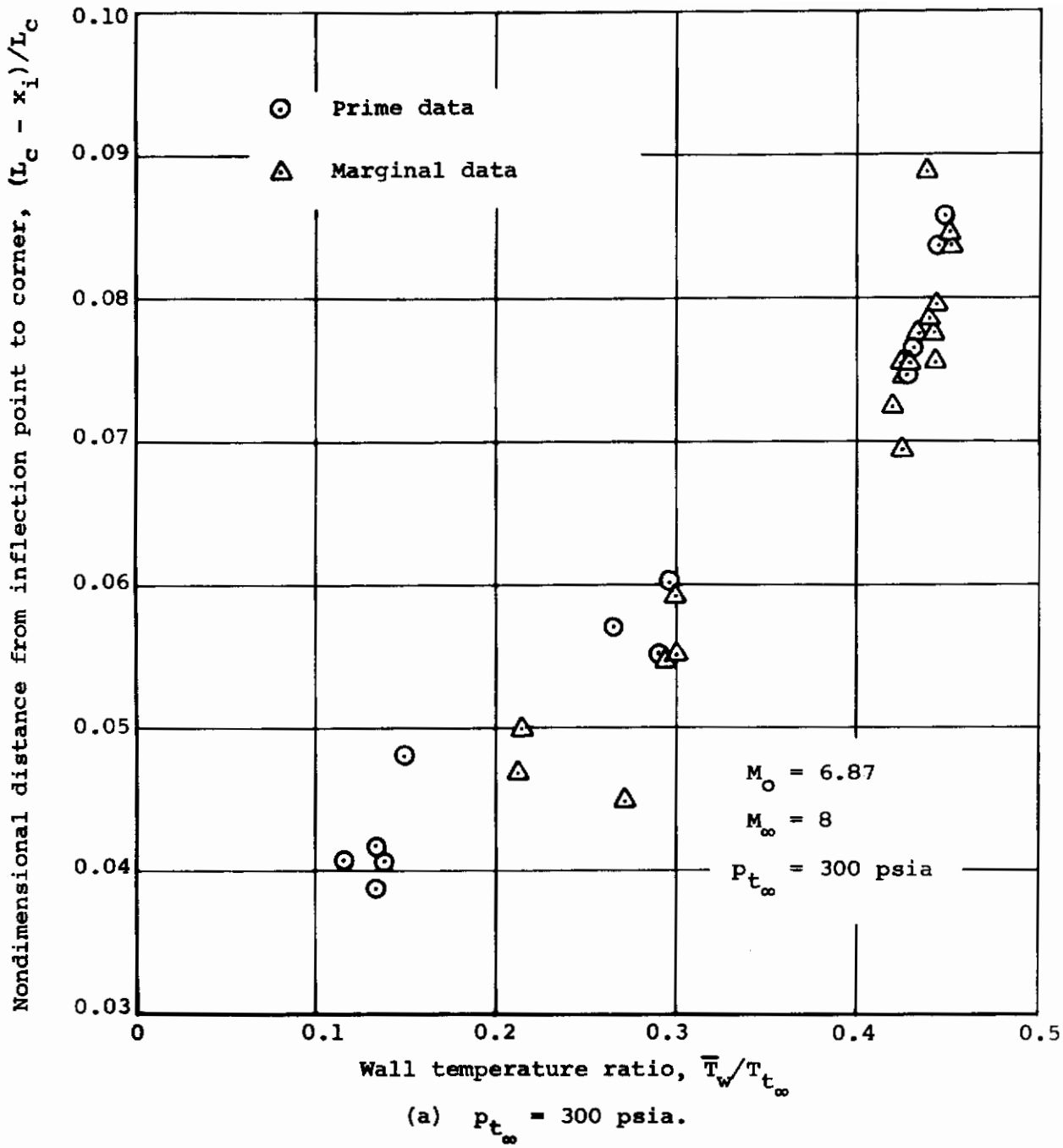

(a) p_{t_∞} = 300 psia.

Figure 7.- Effect of wall temperature ratio on distance between inflection point and corner; prime data and marginal data.

Approved for Public Release

Contrails

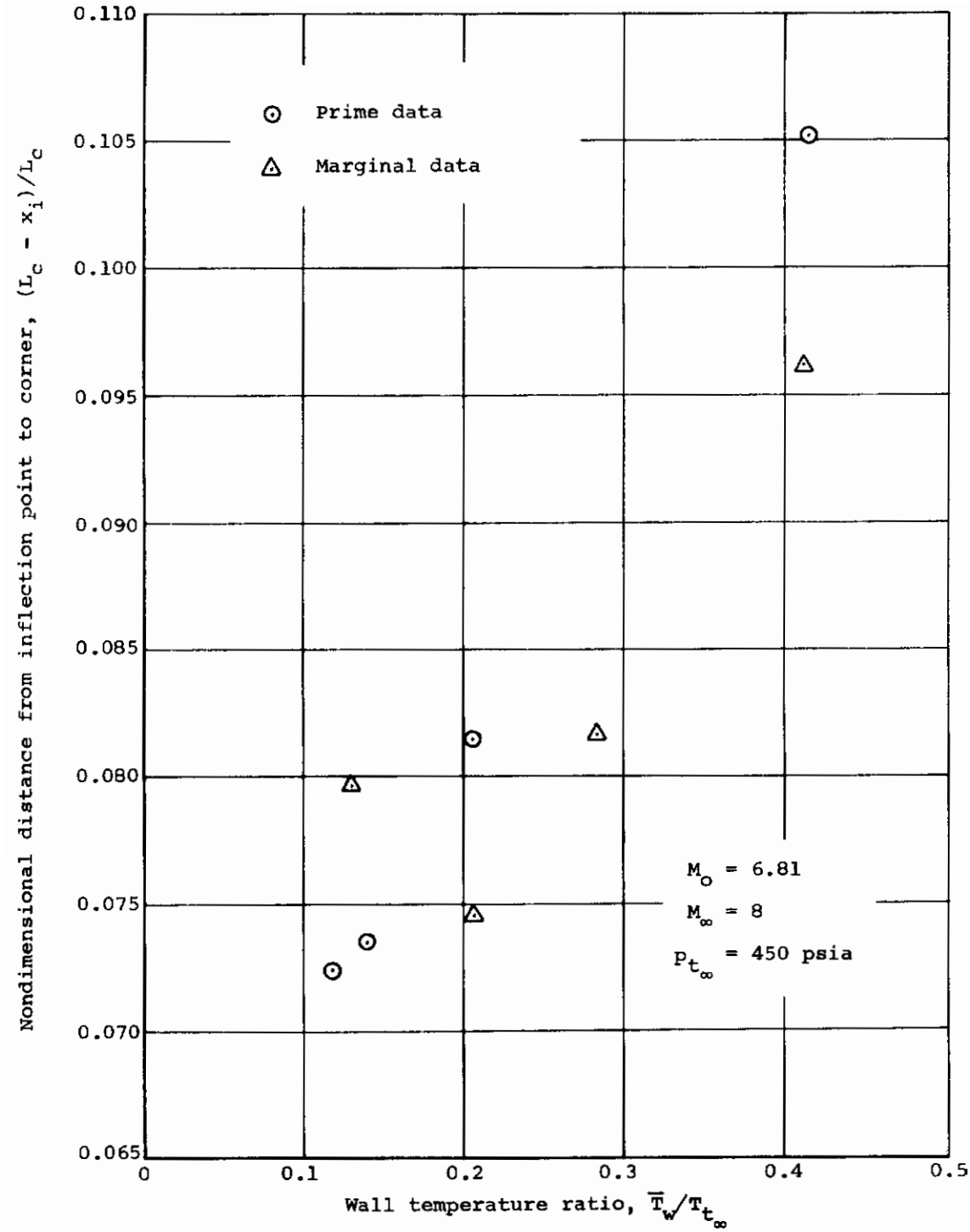

(b) p_{t_∞} = 450 psia.

Figure 7.- Continued.

Approved for Public Release

Contrails

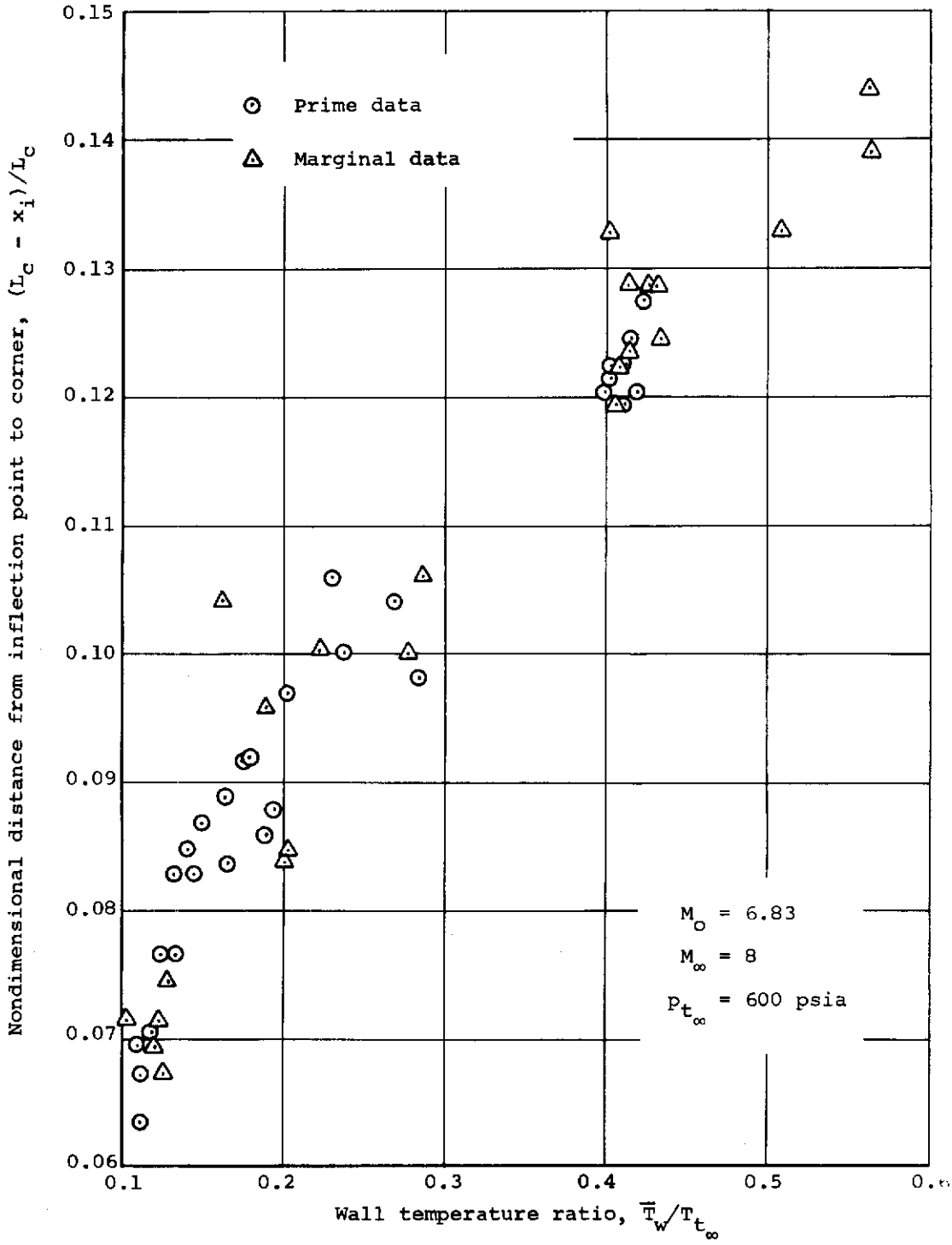

(c) p_{t_∞} = 600 psia.

Figure 7.- Concluded.

Approved for Public Release

Contrails

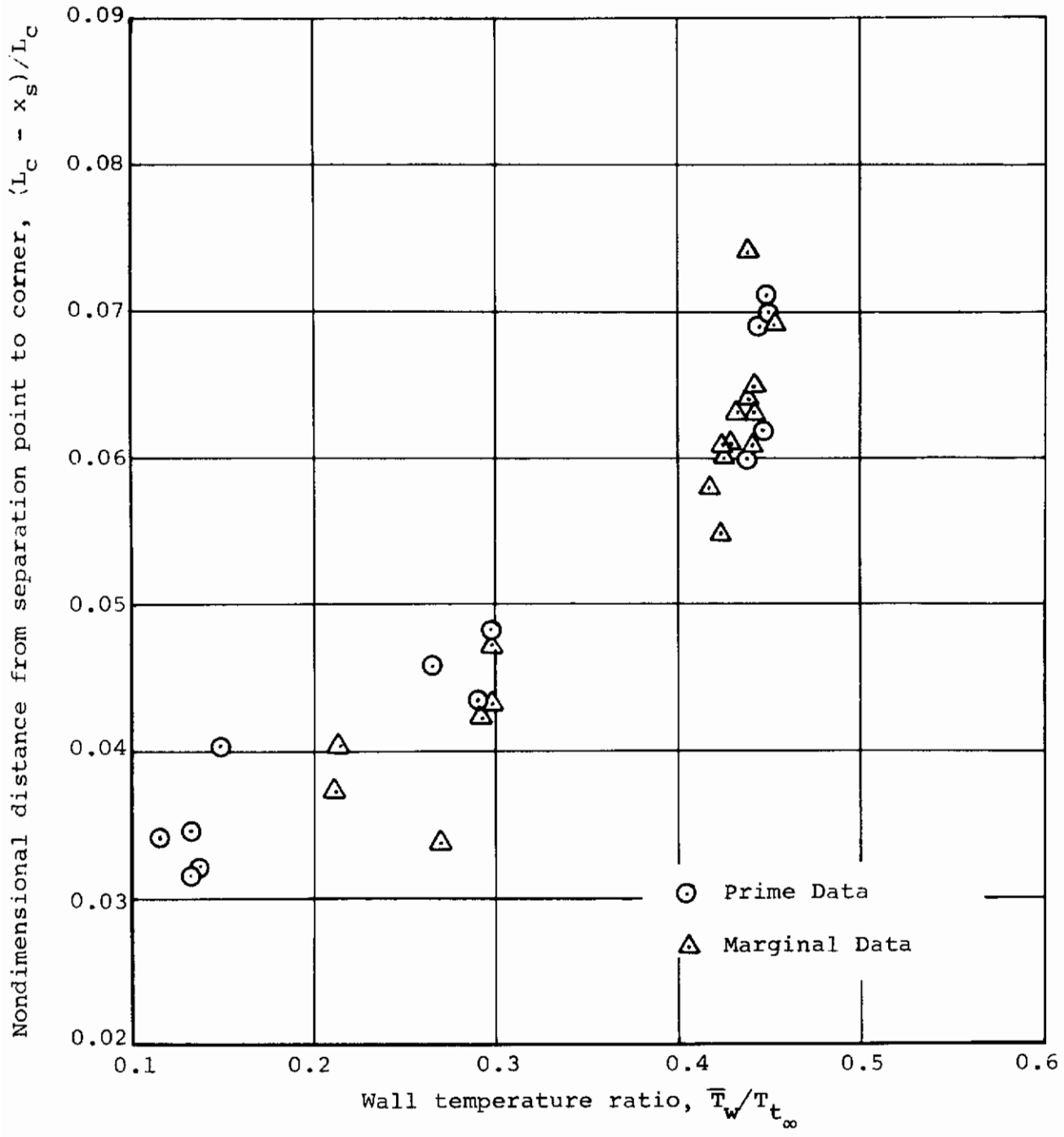

(a) p_{t_∞} = 300 psia.

Figure 8.- Effect of wall temperature ratio on distance between separation point and corner; prime data and marginal data.

Approved for Public Release

Contrails

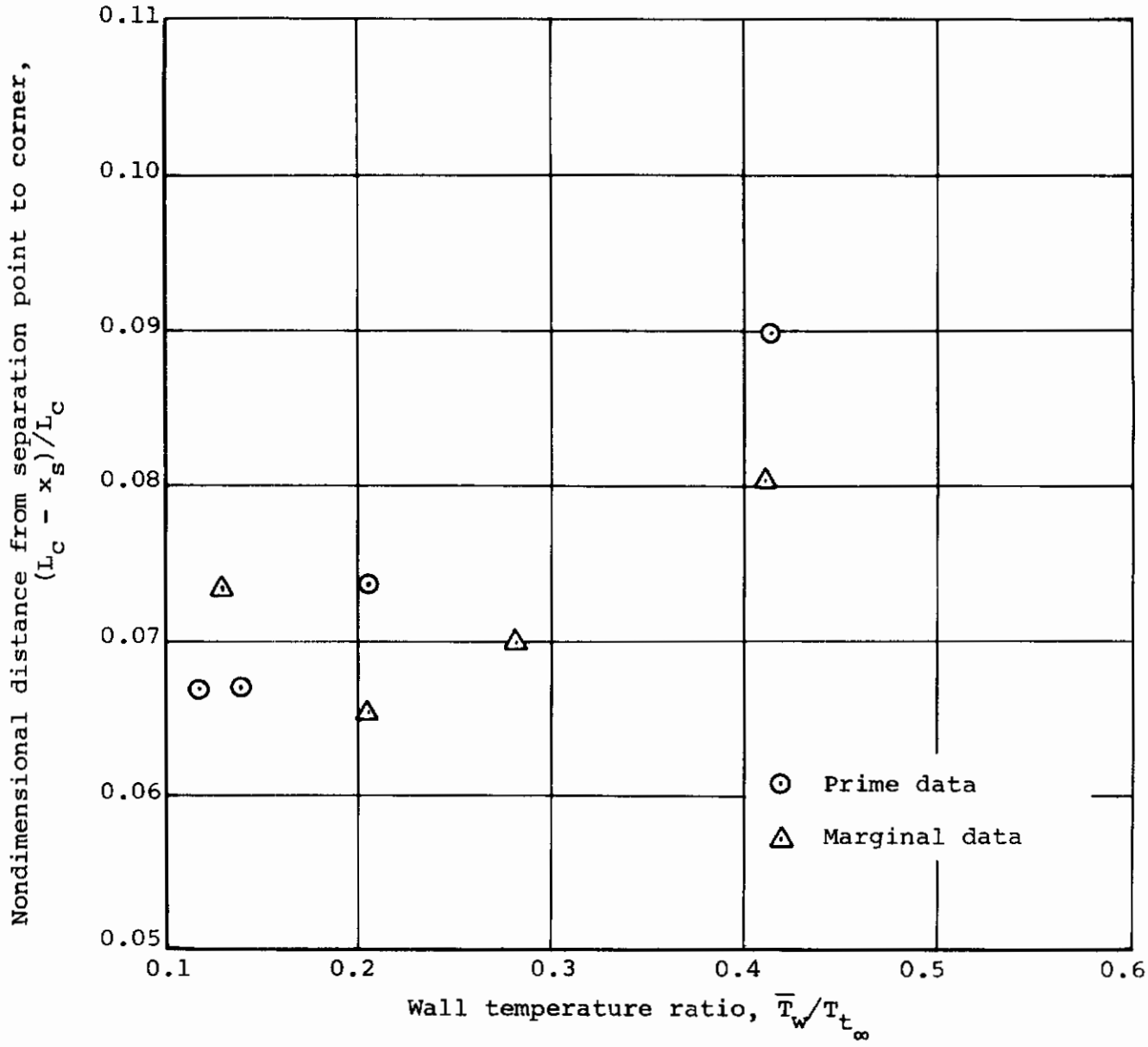

(b) p_{t_∞} = 450 psia.

Figure 8.- Continued.

Approved for Public Release

Contrails

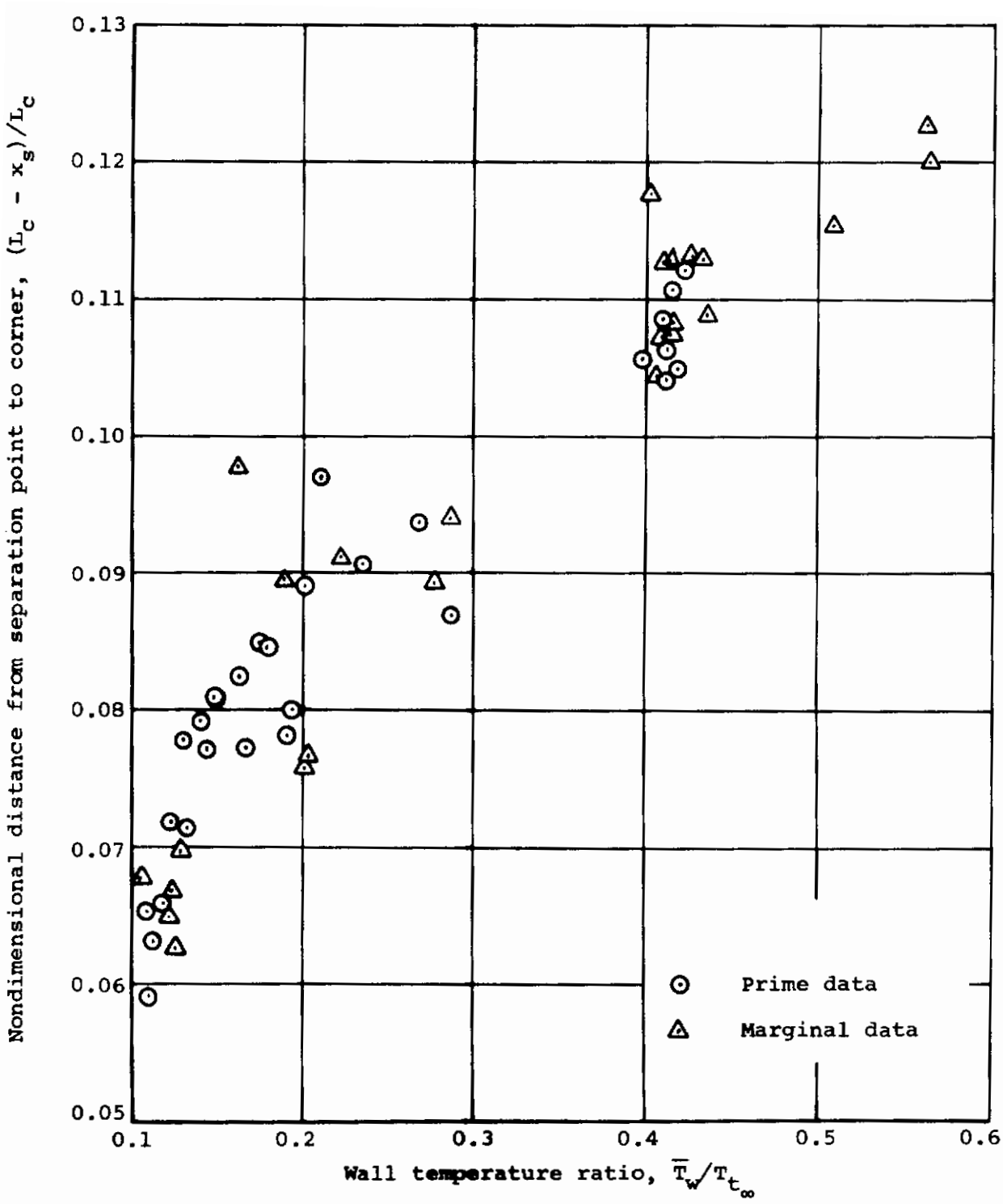

(c) p_{t_∞} = 600 psia.

Figure 8.- Concluded.

Approved for Public Release

Contrails

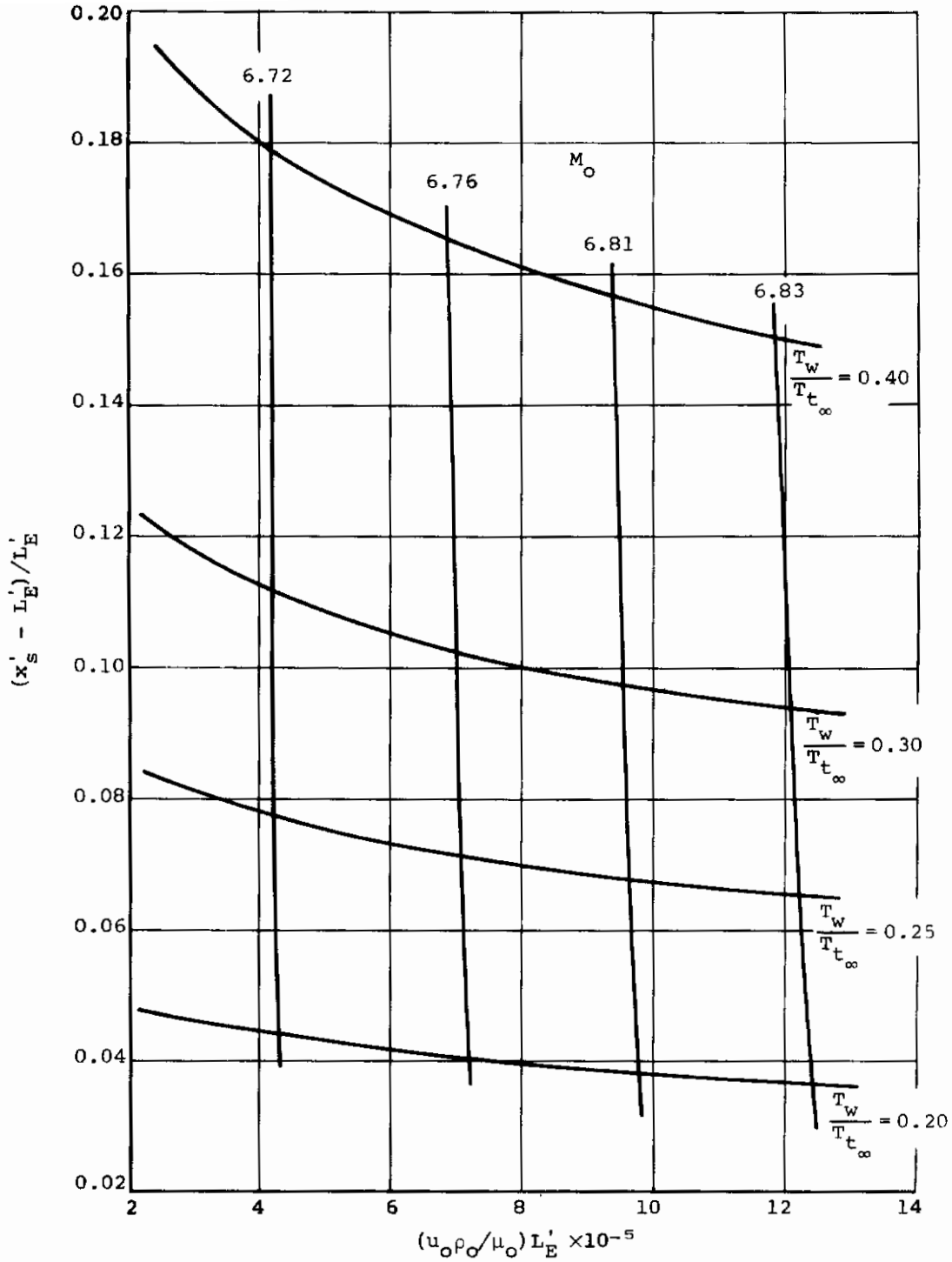

Figure 9.- Theoretical variation of nondimensional distance between the beginning of interaction and separation with initial Reynolds number for fixed temperature ratios.

Approved for Public Release

Contrails

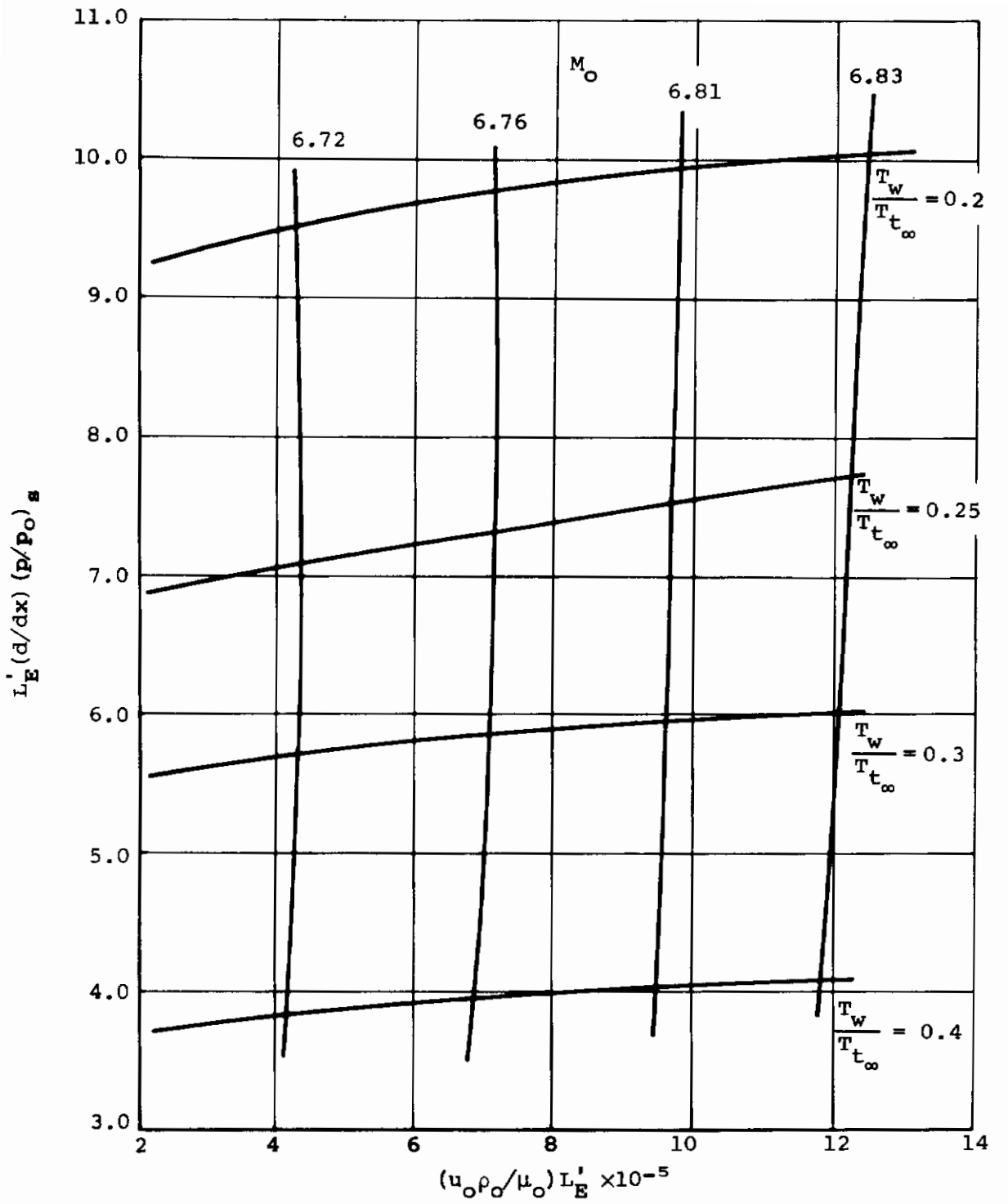

Figure 10.- Theoretical variation of nondimensional pressure gradient at separation with initial Reynolds number for fixed temperature ratios.

Approved for Public Release

Contrails

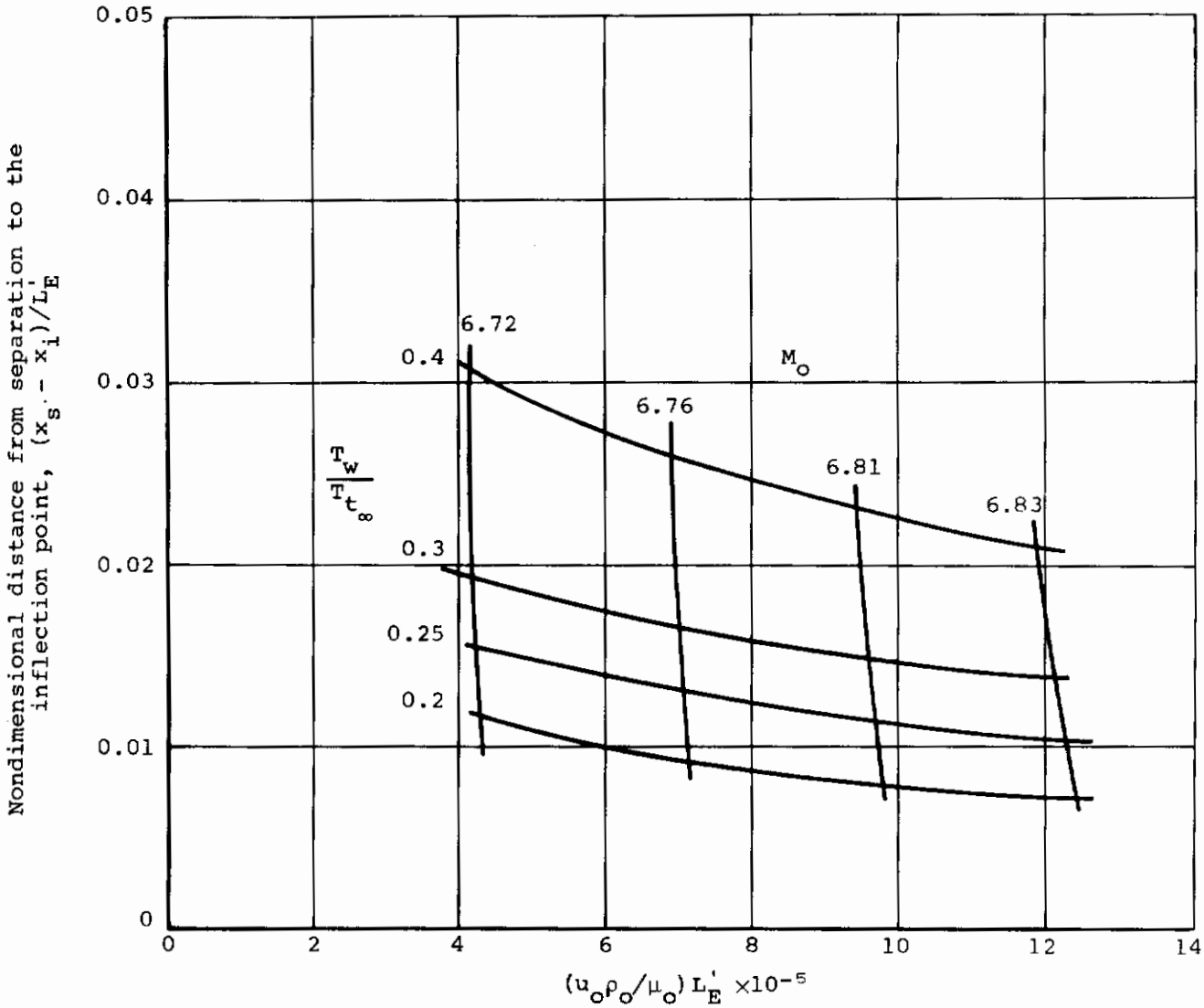

Figure 11.- Theoretical variation of nondimensional distance from separation to the inflection point with initial Reynolds number.

Approved for Public Release

Contrails

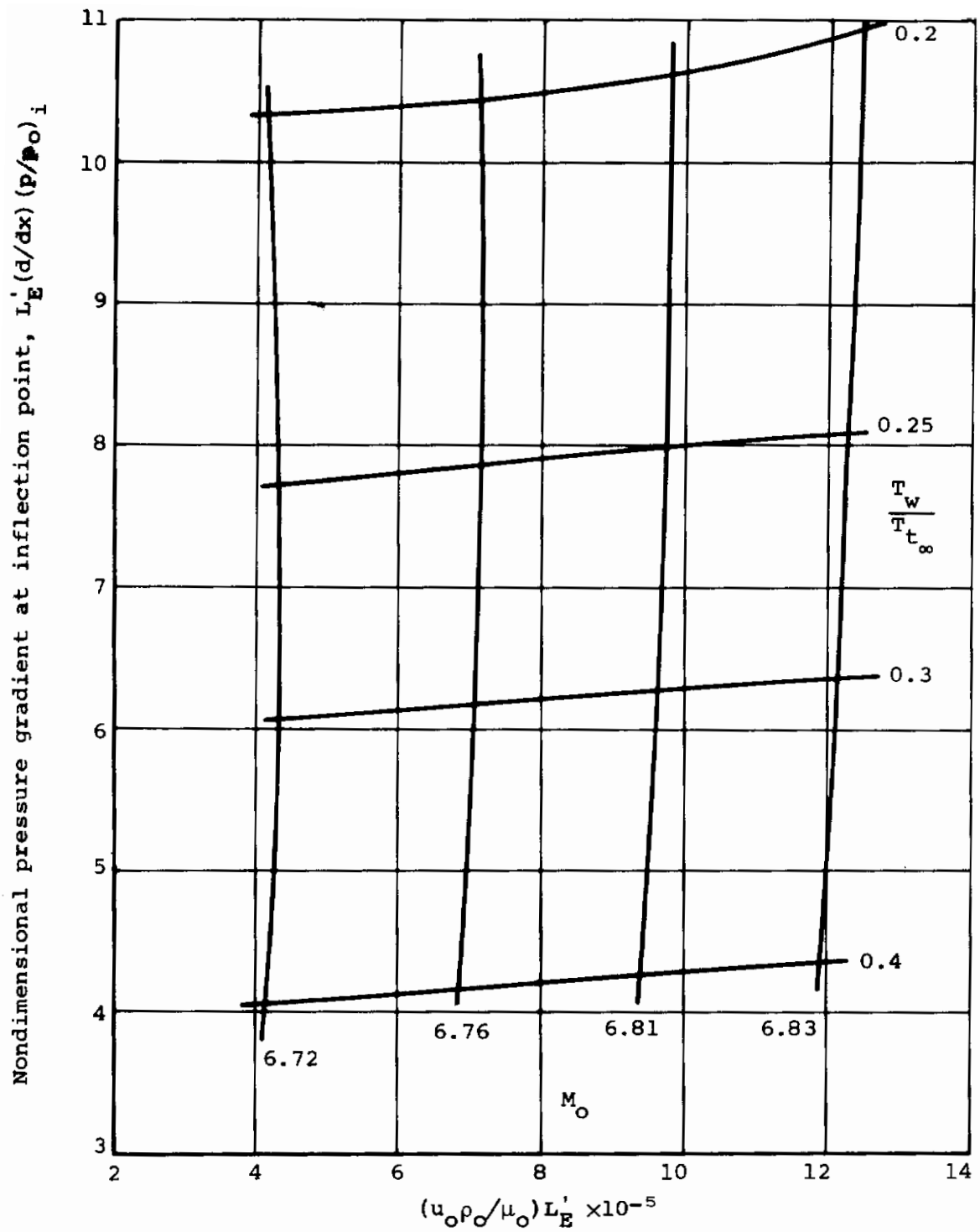

Figure 12.- Theoretical variation of nondimensional pressure gradient at inflection point with initial Reynolds number.

Approved for Public Release

Contrails

APPENDIX

METHOD FOR FITTING THEORY TO EXPERIMENTAL PRESSURE DISTRIBUTION

Consider figure 4 which shows an ogive-cylinder-flare combination and its pressure distribution. The beginning of interaction occurs at point "0" and separation is at point "S". The inflection point "i" is slightly upstream of S in the present sketch. In flow over the body to point 0, the beginning of interaction, the boundary layer is essentially of the Blasius type because of the smooth fairing of the nose into the cylinder and the long cylindrical run at constant pressure. Accordingly, it is described by a Reynolds number designated for a given Mach number and temperature ratio T_w/T_{t_∞} by

$$Re_o = \frac{u_o \rho_o}{\mu_o} L'_E$$

Consider a flat-plate laminar boundary layer with edge conditions u_o, ρ_o, and μ_o. Then L'_E is the boundary-layer run on the flat plate at which the flat-plate boundary layer is identical to that at 0 on the ogive-cylinder-flare combination.

The theory of reference 2 yields the result that all separation lengths and pressures properly nondimensionalized depend only on Re_o, M_o, and T_w/T_{t_∞}. The nondimensional distance from the beginning of interaction to separation, $(x'_s - L'_E)/L'_E$, is such a quantity as well as the nondimensional pressure gradient at separation, $L'_E(d/dx)(p/p_o)_s$. These quantities have been calculated as a function of Re_o for fixed values of the ratio T_w/T_{t_∞} and M_o. The matrix of initial conditions is seen in figure 9, which presents the theoretical variation of $(x_s - L'_E)/L'_E$ as a function of Re_o for various fixed temperature ratios. The value of M_o varies between 6.72 and 6.83 depending on Re_o to allow for the slight experimental variation of p_o/p_∞ with Re_o due to boundary-layer displacement effects. However, the plots are essentially constant Mach number plots since any effects due to these small Mach number differences are also small. A plot is shown in figure 10 for the nondimensional separation pressure gradient $L'_E(d/dx)(p/p_o)_s$, in figure 11 for the nondimensional distance $(x'_s - x_i)L'_E$, and in figure 12 for the nondimensional pressure gradient $L'_E(d/dx)(p/p_o)_i$. It is noted that the nondimensional pressure gradients at separation and the inflection point are nearly equal.

Approved for Public Release

Contrails

In the data-matching method we will match the slope of the pressure distribution at the estimated position of the inflection point (or at the separation point). The quantities $(d/dx)(p/p_o)_i$, u_o, ρ_o, and μ_o are thus given. A trial value of L'_E is specified, and the corresponding Re_o is determined. The value of $L'_E(d/dx)(p/p_o)_i$ is then read from figure 12, and the theoretical value of $(d/dx)(p/p_o)_i$ determined. If the theoretical value does not match the experimental value, then a new trial L'_E is chosen and the calculation repeated.

In comparing data and theory we are at liberty to shift the theoretical curve parallel to itself axially until the data and theory match. We might match theoretical and experimental inflection points, separation points, or beginning of interaction points. If the inflection points are matched, the separation point can be located with the help of the plot of $(x_s - x_i)/L'_E$ presented in figure 11.

The foregoing procedure of data matching is quite general, and requires only that a parametric series of runs be made over the range of the variables of interest. A method of estimating L'_E by boundary-layer theory, rather than empirically as described above, is to be found in reference 14.

Approved for Public Release

Contrails

REFERENCES

1. Lynes, L. L., Nielsen, J. N., and Goodwin, F. K.: Inhibition of Flow Separation at High Speed. Vol. I - Supersonic Turbulent Boundary Layers. Air Force Flight Dynamics Lab. Rep. AFFDL-TR-68-119, Vol. I, Sept. 1968.

2. Goodwin, F. K., Nielsen, J. N., and Lynes, L. L.: Inhibition of Flow Separation at High Speed. Vol. II - Nonadiabatic Laminar Boundary Layers on Flat-Plate-Wedge and Cylinder-Flare Configurations. Air Force Flight Dynamics Lab. Rep. AFFDL-TR-68-119, Vol. II, Sept. 1968.

3. Nielsen, J. N., Lynes, L. L., and Goodwin, F. K.: Calculation of Laminar Separation with Free Interaction by the Method of Integral Relations. Part I - Two-Dimensional Supersonic Adiabatic Flows. Air Force Flight Dynanics Lab. Rep. AFFDL-TR-65-107, Oct. 1965.

4. Nielsen, J. N., Lynes, L. L., and Goodwin, F. K.: Calculation of Laminar Separation with Free Interaction by the Method of Integral Relations. Part II - Two-Dimensional Supersonic Nonadiabatic Flow and Axisymmetric Supersonic Adiabatic and Nonadiabatic Flows. Air Force Flight Dynamics Lab. Rep. AFFDL-TR-65-107, Jan. 1966.

5. Nielsen, J. N., Lynes, L. L., and Goodwin, F. K.: Theory of Laminar Separated Flows on Flared Surfaces Including Supersonic Flow with Heating and Cooling. AGARD Conference Proceedings, no. 4, part I, proceedings of AGARD Fluid Dynamics Panel held in Rhode-Saint-Genése, Belgium, 10-13 May 1966.

6. Ryder, M. O., Jr.: Skin Friction, Heat-Transfer, and Pressure Measurements on Hypersonic Inlet Compression Surfaces in the Mach Number Range 7.6 to 16. AFFDL-TR-65-199, Dec. 1965.

7. Fleeman, E. L.: Incipient Separation for Highly-Cooled Walls in a Hypersonic Free Stream. FDCC TM 66-13, Air Force Flight Dynamics Lab., Dec. 1966.

8. Lankford, J. L.: Effects of Heat Transfer on Laminar Separation on Axisymmetric Compression Surfaces in Hypersonic Flow. Preprint from the Fifth U. S. Navy Symposium on Aeroballistics, NOL, White Oak, Maryland, 16-18 Oct. 1961.

9. Lankford, J. L.: The Effect of Heat Transfer on the Separation of Laminar Flow Over Axisymmetric Compression Surfaces. Preliminary Results at Mach Number 6.78. NAVWEPS Rep. 7402, Mar. 1961.

10. Lankford, J. L.: Investigation of the Flow Over an Axisymmetric Compression Surface at High Mach Numbers. NAVORD Rep. 6866, May 1961.

11. Gray, J. D.: Wall Cooling Effects on Axisymmetric Laminar Reattaching Flows at Hypersonic Speeds. AEDC-TR-68-135, to be published.

12. Gray, J. D. and Prater, W. R.: Initial Experience with a Fast-Response Pressure System for Wind Tunnels with Injection Systems. ARO, Inc., presented at the 29th Supersonic Tunnel Association Meeting, U. S. Naval Ordnance Lab., White Oak, Maryland, Apr. 22-24, 1968.

Approved for Public Release

Contrails

13. Kuehn, D. M.: Experimental Investigation of the Pressure Rise Required for the Incipient Separation of Turbulent Boundary Layer in Two-Dimensional Supersonic Flow. NASA Memo 1-21-59A, Feb. 1959.

14. Abbott, D. E., Holt, M., and Nielsen, J. N.: Investigation of Hypersonic Flow Separation and its Effect on Aerodynamic Control Characteristics. ASD TDR-62-963, Nov. 1962.

Approved for Public Release

Contrails

Approved for Public Release

Contrails

Unclassified
Security Classification

DOCUMENT CONTROL DATA - R&D
(Security classification of title, body of abstract and indexing annotation must be entered when the overall report is classified)

1. ORIGINATING ACTIVITY (Corporate author) Nielsen Engineering & Research, Inc. 3967 East Bayshore Palo Alto, California 94303	2a. REPORT SECURITY CLASSIFICATION Unclassified 2b. GROUP N/A

3. REPORT TITLE

Inhibition of Flow Separation at High Speed
Vol. III - Experimental Results for Laminar Boundary Layers

4. DESCRIPTIVE NOTES (Type of report and inclusive dates)
Technical Documentary Report, Vol. III - Oct. 1966 to Sept. 1968

5. AUTHOR(S) (Last name, first name, initial)
Nielsen, Jack N., Lynes, Larry L., and Goodwin, Frederick K.

6. REPORT DATE	7a. TOTAL NO. OF PAGES	7b. NO. OF REFS
March 1969	60	14

8a. CONTRACT OR GRANT NO. F33615-67-C-1096 b. PROJECT NO. 8219 c. Task No. 821902 d.	9a. ORIGINATOR'S REPORT NUMBER(S) AFFDL-TR-68-119, Vol. III 9b. OTHER REPORT NO(S) (Any other numbers that may be assigned this report) NEAR Report TR 9

10. AVAILABILITY/LIMITATION NOTICES
This document has been approved for public release and sale; its distribution is unlimited.

11. SUPPLEMENTARY NOTES	12. SPONSORING MILITARY ACTIVITY
None	Air Force Flight Dynamics Laboratory Wright-Patterson Air Force Base Ohio 45433

13. ABSTRACT

This report is the third in a series of reports on the subject of inhibition of separation at high speed. It describes the results of a wind-tunnel test program carried out at the von Karman Facility of the Arnold Engineering and Development Center at Tullahoma, Tennessee, on an ogive-cylinder-flare combination to determine the extent of laminar separation as a function of wall temperature for fixed free-stream Reynolds number per unit length at a free-stream Mach number of 8.0. The objective of the tests was to see if separation could be eliminated entirely by cooling the wall to a sufficiently low value.

Pressure and temperature distributions spanning the separation region were made on a quick-insertion model, but the location of the separation point could not be obtained during the tests. Accordingly, a combined experimental-theoretical method was developed for determining the separation point location. Correlation of the separation length with model temperature ratio indicated that the separation distance was small and was rapidly approaching zero at the lowest wall temperature ratio achieved experimentally. The apparent critical wall temperature ratio so indicated by the data was lower than the theoretical ratio. It was not possible to achieve sufficiently low temperatures to see if separation could be entirely eliminated. Possible reasons for the difference between experiment and theory are discussed

DD FORM 1 JAN 64 1473

Unclassified
Security Classification

Approved for Public Release

Contrails

14. KEY WORDS	LINK A		LINK B		LINK C	
	ROLE	WT	ROLE	WT	ROLE	WT
Thermal boundary layer Laminar boundary layer Separated flow Supersonic flow Aerodynamics Aerodynamic heating						

INSTRUCTIONS

1. ORIGINATING ACTIVITY: Enter the name and address of the contractor, subcontractor, grantee, Department of Defense activity or other organization *(corporate author)* issuing the report.

2a. REPORT SECURITY CLASSIFICATION: Enter the overall security classification of the report. Indicate whether "Restricted Data" is included. Marking is to be in accordance with appropriate security regulations.

2b. GROUP: Automatic downgrading is specified in DoD Directive 5200.10 and Armed Forces Industrial Manual. Enter the group number. Also, when applicable, show that optional markings have been used for Group 3 and Group 4 as authorized.

3. REPORT TITLE: Enter the complete report title in all capital letters. Titles in all cases should be unclassified. If a meaningful title cannot be selected without classification, show title classification in all capitals in parenthesis immediately following the title.

4. DESCRIPTIVE NOTES: If appropriate, enter the type of report, e.g., interim, progress, summary, annual, or final. Give the inclusive dates when a specific reporting period is covered.

5. AUTHOR(S): Enter the name(s) of author(s) as shown on or in the report. Enter last name, first name, middle initial. If military, show rank and branch of service. The name of the principal author is an absolute minimum requirement.

6. REPORT DATE: Enter the date of the report as day, month, year; or month, year. If more than one date appears on the report, use date of publication.

7a. TOTAL NUMBER OF PAGES: The total page count should follow normal pagination procedures, i.e., enter the number of pages containing information.

7b. NUMBER OF REFERENCES: Enter the total number of references cited in the report.

8a. CONTRACT OR GRANT NUMBER: If appropriate, enter the applicable number of the contract or grant under which the report was written.

8b, 8c, & 8d. PROJECT NUMBER: Enter the appropriate military department identification, such as project number, subproject number, system numbers, task number, etc.

9a. ORIGINATOR'S REPORT NUMBER(S): Enter the official report number by which the document will be identified and controlled by the originating activity. This number must be unique to this report.

9b. OTHER REPORT NUMBER(S): If the report has been assigned any other report numbers *(either by the originator or by the sponsor)*, also enter this number(s).

10. AVAILABILITY/LIMITATION NOTICES: Enter any limitations on further dissemination of the report, other than those imposed by security classification, using standard statements such as:

(1) "Qualified requesters may obtain copies of this report from DDC."

(2) "Foreign announcement and dissemination of this report by DDC is not authorized."

(3) "U. S. Government agencies may obtain copies of this report directly from DDC. Other qualified DDC users shall request through _____."

(4) "U. S. military agencies may obtain copies of this report directly from DDC. Other qualified users shall request through _____."

(5) "All distribution of this report is controlled. Qualified DDC users shall request through _____."

If the report has been furnished to the Office of Technical Services, Department of Commerce, for sale to the public, indicate this fact and enter the price, if known.

11. SUPPLEMENTARY NOTES: Use for additional explanatory notes.

12. SPONSORING MILITARY ACTIVITY: Enter the name of the departmental project office or laboratory sponsoring *(paying for)* the research and development. Include address.

13. ABSTRACT: Enter an abstract giving a brief and factual summary of the document indicative of the report, even though it may also appear elsewhere in the body of the technical report. If additional space is required, a continuation sheet shall be attached.

It is highly desirable that the abstract of classified reports be unclassified. Each paragraph of the abstract shall end with an indication of the military security classification of the information in the paragraph, represented as *(TS), (S), (C), or (U)*.

There is no limitation on the length of the abstract. However, the suggested length is from 150 to 225 words.

14. KEY WORDS: Key words are technically meaningful terms or short phrases that characterize a report and may be used as index entries for cataloging the report. Key words must be selected so that no security classification is required. Identifiers, such as equipment model designation, trade name, military project code name, geographic location, may be used as key words but will be followed by an indication of technical context. The assignment of links, rules, and weights is optional.

Approved for Public Release